small structures
www.small-structures.com

Microneedle Optimization: Toward Enhancing Microneedle's Functionality and Breaking the Traditions

Elham Lori Zoudani, Nam-Trung Nguyen, and Navid Kashaninejad**

Microneedles hold remarkable potential for providing convenient and unique solutions for disease diagnosis and therapy. However, their integration into clinical practices has been slow, primarily due to the challenge of developing models that meet the criteria of a particular application. A comprehensive and systematic analysis of all aspects of microneedle platforms is imperative to overcome this bottleneck. The analysis involves gathering performance-related information and understanding the factors affecting the functionality of microneedles. The performance of microneedles is heavily influenced by parameters such as dimensions, needle shape, array arrangement, and materials (flexible, stretchable, stimuli-responsive, biodegradable). This article presents a fresh perspective on microneedles, introducing concepts toward optimal designs across various microneedle platforms. This includes application, design, fabrication techniques, and understanding how a specific microneedle design can effectively meet the requirements of a particular application. By addressing these crucial issues, further advancement of microneedle technology occurs.

1. Introduction

Microneedles represent a novel class of microdevices with widespread applications spanning biomedical to agricultural fields.[1–5] Their capability as a painless, bloodless drug delivery or biosensing device has been explored for years.[6–11] Using microneedles primarily involves delivering a precise amount of drug at a specific rate to a designated location in drug delivery applications. Additionally, they excel with precise sensing in point-of-care diagnostics, ensuring minimal discomfort caused by contact with nerve endings and blood capillaries.[12]

Their unique ability to disrupt only outer tissue layers enhances task efficiency compared to alternative delivery methods. Microneedles may take various shapes[13–19] and be fabricated from various materials,[20–23] offering flexibility and versatility. The effectiveness of microneedles is intricately tied to the chosen shape and material, further emphasizing their significance in microdevice applications.

A well-designed microneedle device tailored to a specific application is crucial before initiating the fabrication process. The primary step involves gaining a comprehensive understanding of the factors influencing the functionality of these devices. It is important to acknowledge that these parameters may vary across applications. However, the convenience and compatibility of these devices with body parts, with zero patient risks, is the constant property that should be met across all applications.

In biomedical applications, clinical considerations and expectations are vital for designing microneedles. Careful consideration must be given to various design criteria, including the type and shape of microneedles, materials used, and fabrication methods. The shape of microneedles determines their efficacy in drug delivery, sensing, or mechanical insertion performance,[24–26] The selected materials play a crucial role in achieving a patch with adequate mechanical strength and appropriate delivery style for therapeutic applications[27,28] or effective diagnosis for in situ biosensing.[29,30] Additionally, manufacturing parameters significantly influence the features of the fabricated microneedles.[31] These interdependent factors necessitate well-thought-out consideration and solutions before proceeding with the preparation stage. Nevertheless, prioritizing one criterion may affect the selection of others.

The widely recognized form of microneedles is a uniform array of plain conical structures positioned perpendicular to a solid patch. This traditional design has found extensive applications across various fields. However, nonconventional designs may enhance performance and potentially overcome the limitations of the above-traditional design. The motivation behind creating new microneedle designs stems from the desire to achieve three primary objectives: 1) optimal therapy or biosensing, that is, improving the effectiveness of drug delivery or biosensing capabilities through new designs; 2) high tissue adhesiveness, that is, attaching securely to the tissue, ensuring stability during application; and 3) effective microneedle mechanical insertion, that is, ensuring mechanical strength, minimizing insertion force, and achieving the deepest possible penetration depth. These objectives drive the exploration of innovative designs beyond the traditional, aiming to elevate the overall functionality and performance of microneedle applications.

E. Lori Zoudani, N.-T. Nguyen, N. Kashaninejad
Queensland Micro- and Nanotechnology Centre, Nathan Campus
Griffith University
170 Kessels Road, Brisbane QLD 4111, Australia
E-mail: nam-trung.nguyen@griffith.edu.au;
n.kashaninejad@griffith.edu.au

The ORCID identification number(s) for the author(s) of this article can be found under https://doi.org/10.1002/sstr.202400121.

DOI: 10.1002/sstr.202400121

Over years of research on microneedle array systems, numerous experimental studies have focused on enhancing microneedle performance by introducing new designs from the perspectives of morphology[25,32–34] and material properties,[35–37] addressing the limitations of previous designs. Some researchers have shifted from experimental studies to mathematical modeling and numerical simulations.[38–41] These tools support experiments by offering a cost-effective and time-efficient way to develop a clear vision of an efficient model before the fabrication stage, pushing microneedle technology toward a more desirable platform.[42] This aspect is not the focus of the current study.

Several review studies have explored and reviewed nontraditional design approaches from various aspects. Makvandi et al. researched bioinspired microneedles, emphasizing the incorporation of special functions borrowed from natural creatures in the design of these innovative microneedle systems.[43] Parhi reviewed the advancements in microneedle design for drug delivery and cosmeceutical applications.[44] Jia et al. investigated critical factors in the morphology of polymeric microneedles, considering the respective applications.[19]

The present review aims to provide a unique perspective on the design approach for microneedles, emphasizing the enhancement of their functionality. Our systematic study specifically examines the influence of physical features on the performance of microneedles in the clinical setting. We consider three pivotal aspects: application, design, and fabrication, mainly how the structural characteristics address the requirements of these aspects and how a specific issue can be approached differently. This variation in addressing a single criterion is what we seek to gather and present in this review study.

Figure 1 schematically illustrates the scope of the current review, which is organized into six sections. The introduction briefly provides an overview of microneedles, exploring the parameters affecting their function and underscoring the potential impact of introducing new microneedle designs. Section 2 reviews the role of microneedle designs in drug delivery, biosensing, and tissue adhesion applications. Section 3 highlights the fundamental principles of microneedle design, focusing on mechanical insertion performance. Section 4 covers the fabrication techniques employed for making these microdevices. The challenges these systems face and a future perspective on this field are discussed in Section 5.

2. Application

2.1. Drug Delivery

Several fundamental principles shape the efficacy of microneedle-based drug delivery systems, including the duration of drug release, release patterns, delivered quantity, and, most importantly, the convenience of the process. Understanding the factors affecting the functionality is a crucial initial step. Notably, it has been established that the physical properties of microneedles play a crucial role in determining the effectiveness of a drug delivery system. Carefully selecting the shape and the materials used to fabricate microneedles is essential to address upcoming challenges effectively. Over the past few decades, various microneedle array designs have been proposed to create systems with desired outcomes.[45–47] These designs optimize drug delivery by considering the specific physical characteristics of microneedles.

Figure 2 schematically shows the topics discussed in the following subsections on factors affecting the functionality of microneedles for drug delivery applications.

2.1.1. Microneedle Drug Delivery Systems with Separable Backing Patch Substrate

In drug delivery applications, the choice between burst release and continuous sustained delivery depends on the therapy's site of action and purpose.[48] Note that this selection directly affects the patch wear period. For long-term sustained microneedle-based drug delivery, the necessity of wearing the patch throughout the entire process compromises the convenience offered by these devices.[49] Therefore, there is a demand for a platform that can eliminate this issue. To address this challenge, Li et al. introduced a method for achieving sustained, self-administered drug delivery.[50] They used a rapidly separable, biodegradable microneedles patch to deliver levonorgestrel, a contraceptive hormone. Microneedles were fabricated using biodegradable poly (lactic-*co*-glycolic acid) (PLGA) and polylactic acid (PLA), with safe, water-soluble polyvinyl alcohol (PVA) and sucrose used for the backing substrate. The microneedles featured bubble-shaped structures at the needle–substrate interface, **Figure 3**A. The patch was engineered to withstand compression during microneedle penetration but detach under the sheer force of 0.05–0.08 N needle^{-1}. Upon detachment, the levonorgestrel-loaded microneedles underwent sustained degradation, enabling systemic hormone delivery for over a month. The bubble-microneedle array patch effectively maintained the levonorgestrel concentration above the human therapeutic level of 200 pg/ml for one month in tested rats. This delivery system offers a safe and effective platform for the long-term delivery of levonorgestrel, a hormone with an extensive history of clinical contraceptive applications.

In continuation of the studies done on fabricating patches with the separable supporting substrate,[51] Kim et al. developed a patch of bioresorbable, miniaturized porous–silicon (p-Si) needles on a temporary, flexible, water-soluble baseplate for sustained delivery of chemotherapeutic drugs.[52] Using the flexible backing substrate improved the microneedle's adherence to the cornea. The water-soluble base film was used temporarily for insertion. It dissolved within 1 min of exposure to saline solution, leaving the p-Si needles embedded in the tissue. These microneedles gradually degraded, resulting in sustained drug release.

2.1.2. Microneedle Drug Delivery Systems with Unique Morphology

As mentioned earlier, the amount of drug delivered, the administration site, and the release pattern are crucial criteria for a drug delivery platform. However, one limitation of microneedles is their small size, hindering their ability to deliver high doses.[53,54] Overcoming this limitation and ensuring sufficient drug administration necessitates an increase in the drug-carrying capacity of microneedles. Microneedle morphology is pivotal in addressing this challenge, allowing for transformative enhancements. Ohn et al. introduced the concept of "candlelit"-shape dissolving

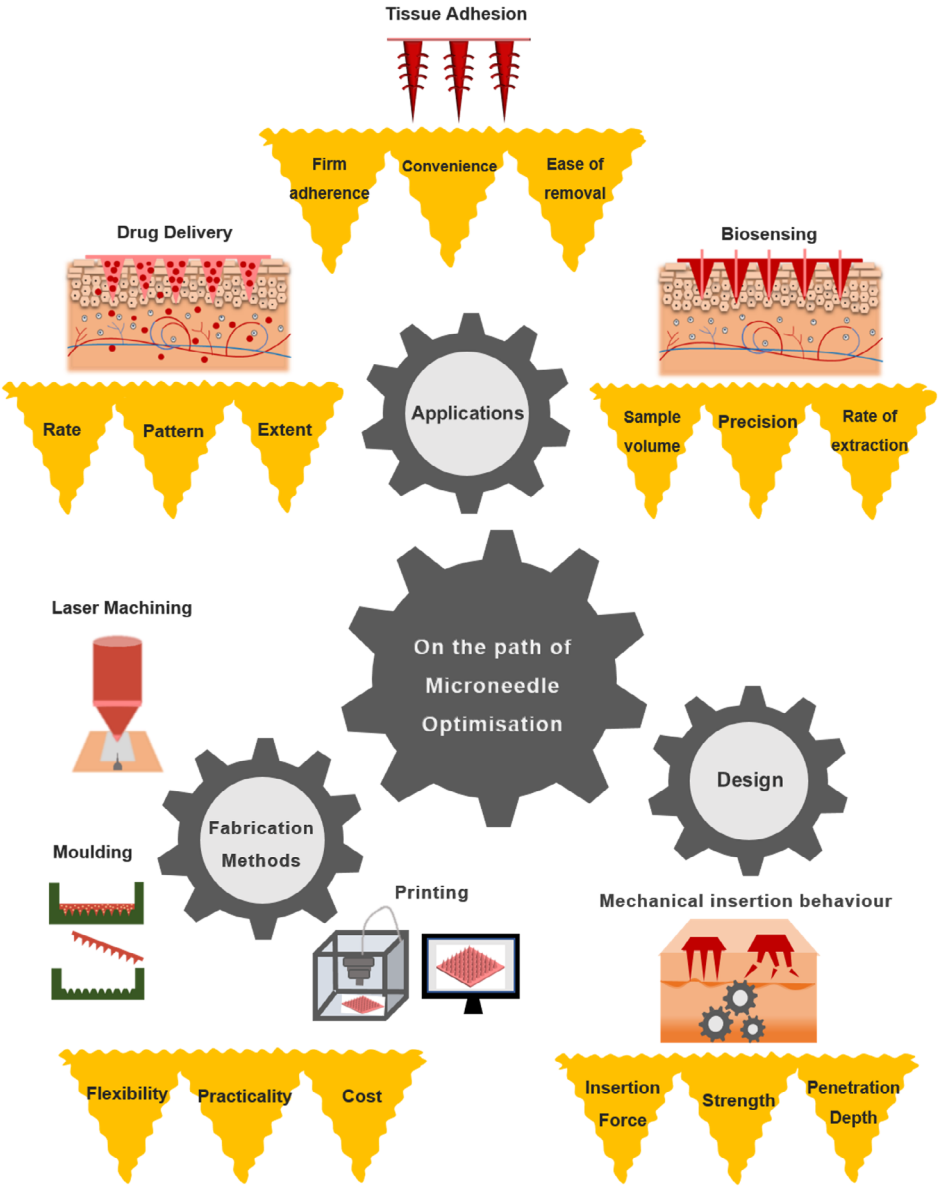

Figure 1. Scope of the review toward microneedle optimization. Principles involved in determining the optimum design of all aspects of microneedles, application, design, and fabrication techniques. Schematic of the tissue anatomy in drug delivery and biosensing parts is redrawn with some changes from ref. [115], Copyright 2020, Elsevier.

microneedles loaded with triamcinolone acetonide, an anti-inflammatory steroid drug (Candlelit-DMN).[55] Utilizing a specialized applicator for insertion, these microneedles exhibited deeper penetration than conventional conical shapes. The unique candlelit morphology facilitated the delivery of a larger drug quantity deeper into the tissue, ensuring a more even distribution of drug release. In vivo, the skin inflammation mouse model highlighted the effectiveness of candlelit dissolving microneedles. These microneedles alleviated inflammation by suppressing inflammatory cell infiltration and cytokine gene expression, achieving results comparable to triamcinolone acetonide intralesional injection (TAILI).

In another approach, Huang et al. drew inspiration from the hierarchical structure of a Christmas tree to design a patch containing two-layer microneedles, as shown in Figure 3B.[56] Loaded with four chemotherapy drugs (fluorouracil, leucovorin, irinotecan, and oxaliplatin), the patch aimed at achieving combination chemotherapy for pancreatic cancer treatment. The two-layer microneedles enabled spatial and temporal release of multiple drugs, providing a means for effective combination chemotherapy in treating pancreatic cancer.

2.1.3. Microneedle Drug Delivery Systems with Smart Stimuli-Responsive Materials for Controlled Release

Significant efforts have been invested in developing smart stimuli-responsive microneedle arrays to achieve controlled

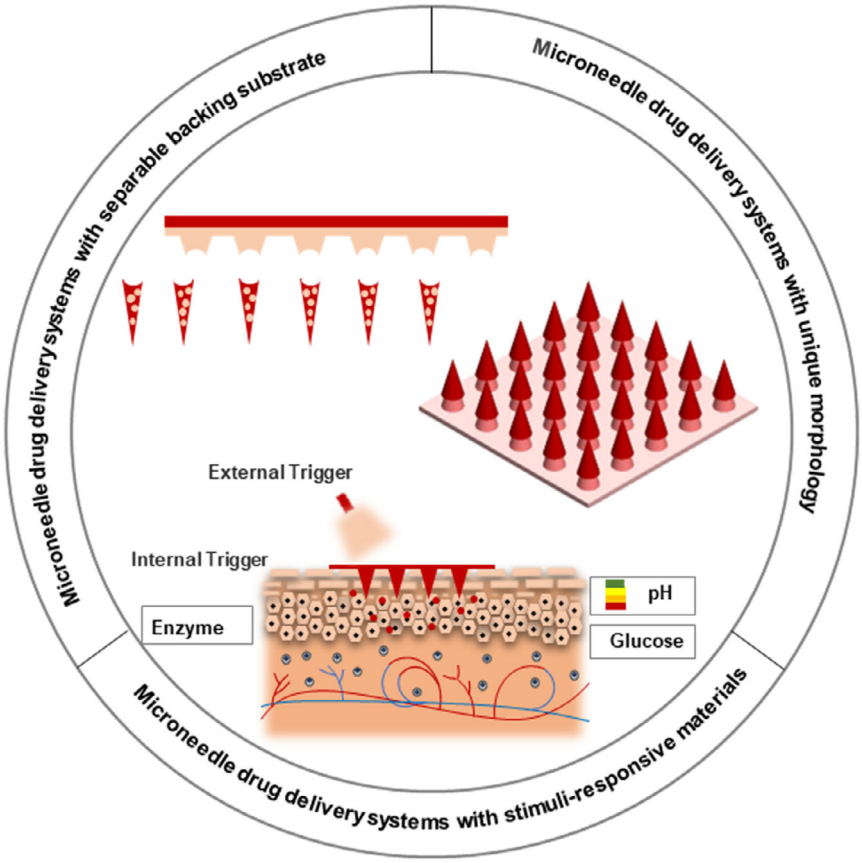

Figure 2. Schematic of the microneedle drug delivery systems with unique morphology was redrawn with some changes from ref. [56], Copyright 2022, AAAS.

drug release. These microneedles are primarily fabricated from smart materials that exhibit responsive behavior when exposed to stimuli, which can be either internal or external.[57] External stimuli, such as light[58] and ultrasound,[59] are applied externally to trigger the microneedles to respond and then release drugs on demand. Conversely, when triggered by internal stimuli such as body temperature,[60] enzymatic reactions,[61] or changes in pH,[62,63] microneedles initiate controlled drug delivery in response to these internal changes.

The body's pH changes in the presence of abnormalities such as cancerous tumors, infections, and inflammations.[64,65] Accordingly, Li et al. designed a pH-responsive gene-loaded microneedle patch to suppress tumor growth through gene delivery.[66] The microneedles were constructed using polycaprolactone (PCL), with pH-responsive polyelectrolyte multilayers (PEM) applied to their surface through a layer-by-layer assembly technique. This PEM incorporated a charge-reversible polymer, dimethylmaleic anhydride-modified polylysine (PLL-DMA), divided into transition layers $(\text{PLL-DMA/polyethyleneimine})_{12}$ and gene-loaded layers $(\text{p53 expression plasmid/polyethyleneimine})_{16}$. The resulting microneedle patch, referred to as tr-MNP, could carry 31 μg of DNA, leading to improved gene release. Comparative experiments with microneedle patches lacking transition layers (ntr-MNP) showed that tr-MNP released 33% of the model DNA in a simulated skin-like environment (phosphate buffer saline; pH = 5.5), while ntr-MNP released only 4%. In vivo experiments demonstrated that tr-MNP-treated mice achieved a tumor inhibition efficacy of 90.1%, surpassing ntr-MNP-treated mice (46.4%) and mice receiving intravenous administration (30.5%).

2.2. Biosensing

Microneedles have emerged as a powerful option for biosensing, offering significant advantages over traditional blood-sampling approaches.[67–69] These tiny needles provide a fast-reporting, convenient, and cost-effective platform for real-time detection of biomarkers.[70] There are two primary strategies for biomarker detection using microneedles. The off-site strategy involves extracting interstitial fluid (ISF) using microneedles and analyzing it separately.[71,72] Conversely, the continuous on-site strategy involves microneedles detecting, capturing, and analyzing biomarkers directly at the application site.[33,73] Developing a reliable microneedle platform for accurate sensing and analysis has been challenging.

Figure 4 schematically illustrates the topics discussed in the following sections on design criteria involved in the functionality of microneedles as biosensors.

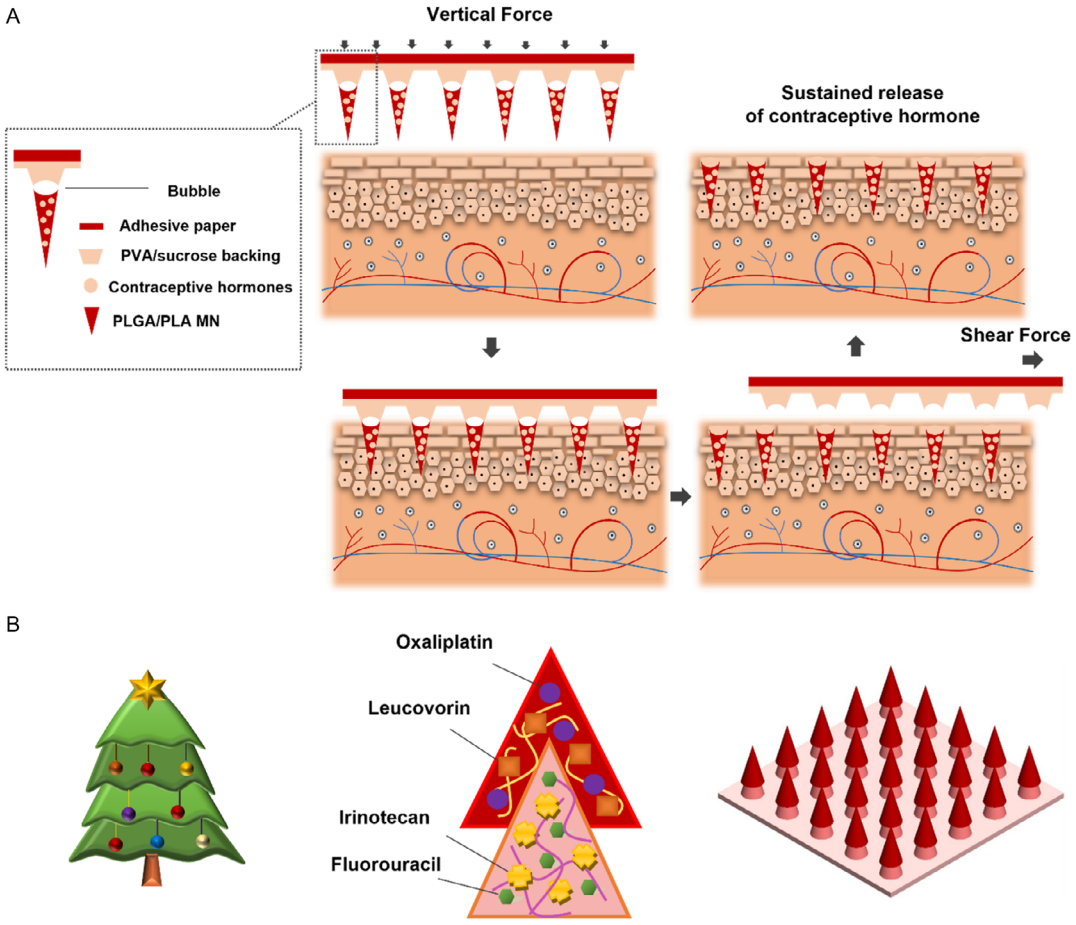

Figure 3. A) Schematic of the administration process of levonorgestrel-loaded microneedles with bubbles in their structure and rapid separation of microneedles from the supporting substrate. Redrawn with some changes from ref. [50], Copyright 2019, Nature. B) Christmas tree-inspired two-layer microneedle for combination chemotherapy. Redrawn with some changes from ref. [56], Copyright 2022, AAAS.

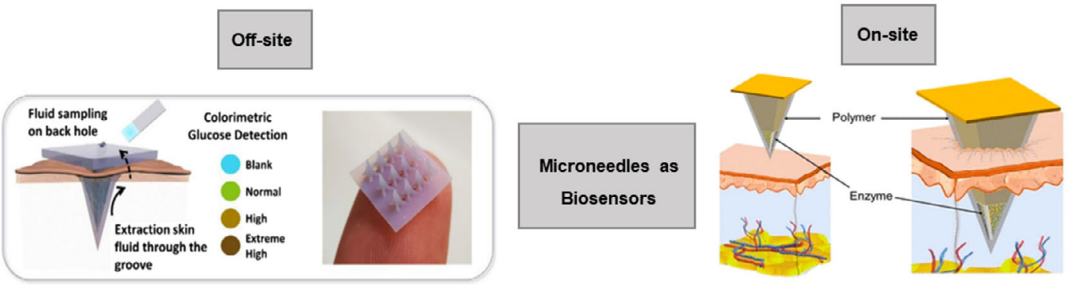

Figure 4. Schematic of topics discussed in the following subsections on design criteria involved in the functionality of microneedles as biosensors. Reprinted with permission.[75] Copyright 2021, Wiley. Reprinted with permission.[76] Copyright 2023, ACS Publications.

2.2.1. Off-Site Biosensors

For off-site microneedle-based sensors, ensuring diagnostic sensitivity depends on maintaining the stability of biomarkers and providing an adequate sample to minimize errors.[74] Therefore, in biomarker diagnosis using microneedle devices, the capability to safely and rapidly obtain sufficient ISF is crucial. Fast sample extraction not only preserves its integrity but also improves patient compliance.[74] Furthermore, ample fluid sample expands the range of applicable biomarkers, enhancing the versatility and utility of microneedle-based biosensors. The combination of rapid extraction speed and sufficient sample volume is pivotal for the success and effectiveness of biomarker diagnosis using microneedle devices.[74]

The design of the microneedles plays a crucial role in determining how fast and efficiently the tissue fluid can be collected. The structure needs to facilitate easy and preferably rapid extraction from the tissue. A tilted microneedles ISF collecting system (TMICS) was proposed to uniformly extract a large amount of ISF at high speed by increasing the exposed surface area of microneedles with the tissue.[74] The design of TMICS aimed to increase the contact area between the microneedles and the tissue while reducing penetration depth compared to the conventional vertical style, as shown in **Figure 5**A. The microneedles were inserted at an angle of 66°, reducing penetration depth and subsequent pain while improving the contact surface between the microneedles and the tissue. The team demonstrated the collection of 2.9 μL of ISF in 30 s. This demonstrates the capability of this design in fluid extraction in such volume in this short period.

Continuing with studies on designing off-site microneedle-based sensors, a patch featuring a groove-channelled microneedle design structure was developed for sampling purposes, as shown in Figure 5B.[75] These microneedles were explicitly designed to facilitate the vertical flow of fluid through channels, from the tip to the baseplate, driven by the generated capillary force. According to their findings, an array of 3×4 microneedles could extract 20–30 μL of body fluid without any absorbent materials. Introducing a structure with this morphology, capable of providing passive capillary-driven fluid flow, allows it to function independently of any additional equipment for fluid extraction and collection, thereby reducing platform complexity.

2.2.2. On-Site Biosensors

In the context of on-site microneedle-based biosensors, ensuring the full functionality of microneedles after insertion is crucial for providing accurate responses during the entire diagnosis process. A significant challenge in maintaining microneedles'

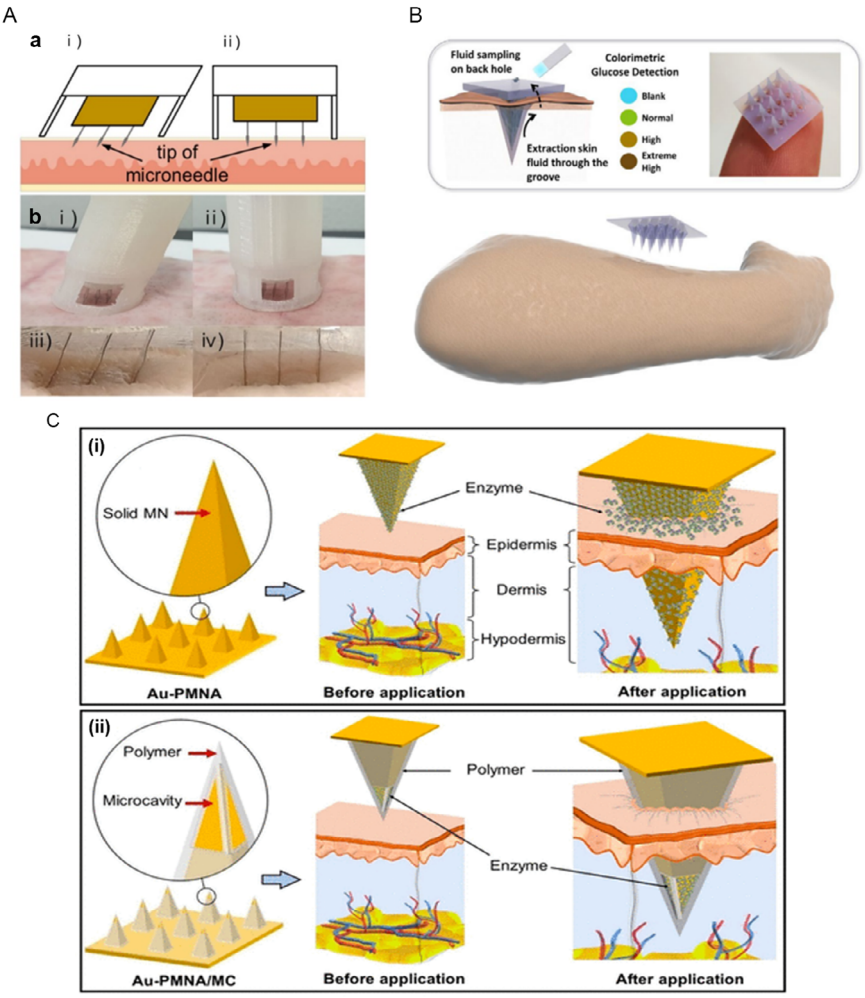

Figure 5. A) (a) Schematic illustration of (i) TMICS. (ii) Straight microneedle ISF collecting system. (b) Digital images of (i) TMICS. (ii) Straight microneedle ISF collecting system. (iii) Penetrated skin by tilted microneedle. (iv) Penetrated skin by straight microneedle collecting system. Reprinted with permission.[74] Copyright 2021, Nature. B) Schematic view of the groove-shaped microneedle array system. Reprinted with permission.[75] Copyright 2021, Wiley. C) Schematic illustration of (i) Au-coated polymeric microneedles and (ii) Au-coated microneedles with recessed microcavities in their structure and penetration procedure into skin layers. Reprinted with permission.[76] Copyright 2023, ACS Publications.

functionality involves safeguarding the biological recognition elements, constituting the sensing layer covering the needle surface, from damage or denaturation. This damage may result from the friction between the microneedle surface and the tissue layers during the insertion and removal processes.[76] To address this challenge, Dervisivic and Voelker introduced a new shape for pyramidal polymeric microneedles featuring recessed microcavities located at the surface tip.[76] These microneedles were designed with recessed microcavities to reach deeper skin layers and access ISF more effectively, as shown in Figure 5C. The sensing layer, containing recognition elements, was accommodated in these microscale pockets to provide complete protection against any delamination or denaturation that might occur during the insertion process. Their study demonstrated that the functionality of the microneedles could be retained even after multiple insertion and removal trials.

2.3. Tissue Adhesion

Despite the numerous advantages of microneedles for therapeutic and sensing purposes, maintaining the patch's adhesion to the tissue for an extended period is a significant challenge. Due to the inherent properties of body tissue, such as tension and repulsion, microneedles tend to be unstable on the tissue and cannot adhere tightly without external support.[77] This challenge becomes especially problematic for microneedle patches on moving parts of the body, where the unique local morphology and functionality may cause the microneedle array to fall off from the surface, leading to partial insertion and potentially impairing the entire process. Therefore, ensuring the tissue adhesiveness of microneedle patches is essential for successful long-term drug delivery or biosensing applications. Approaches to enhance the tissue adhesiveness of microneedles are as follows. 1) *Swelling microneedles:* These microneedles rely on the water absorption capabilities of the needles. Once they penetrate the tissue, the hydrogel-based needles absorb body fluids and expand quickly, resulting in complete tissue interlock.[78,79] 2) *Adhesive materials:* Using adhesive materials, such as chitosan gel, tannin gel, and polydopamine gel, the microneedle supporting substrate can help fix the patch firmly in the intended place.[80–82] 3) *Unique morphological designs:* Inspired by natural creatures, microneedles with unique morphological structures have been developed.[83,84] These designs aim to increase the chances of mechanically interlocking the needles into the tissue layers.

The following sections elaborate on the recent advancements in adhesive microneedles.

Figure 6 schematically illustrates topics discussed in the following subsections on design criteria involved in tissue adhesive microneedles.

2.3.1. Tissue-Adhesive Microneedles with Bioinspired Morphology

Over a million years of evolution, nature has provided a rich source of creatures that have successfully adapted and survived through a continuous and evolving natural selection process. Researchers have gained valuable insights into unique design and functional features by closely observing and studying these natural structures.[85–87] An example is the wettability of surfaces, playing a crucial role in applications such as water harvesting,[88,89] antifogging,[90,91] and droplet manipulation.[92,93] With their unique wettability behavior, plant leaves have inspired the development of various superhydrophobic and superhydrophilic surfaces.[94]

Biomimicry and bioinspired engineering extend to microneedle systems as well. Inspired by natural creatures, various microneedles have been developed with unique morphological structures. By mimicking these nature-based designs, the primary goal is to transform the functionality of microneedles to

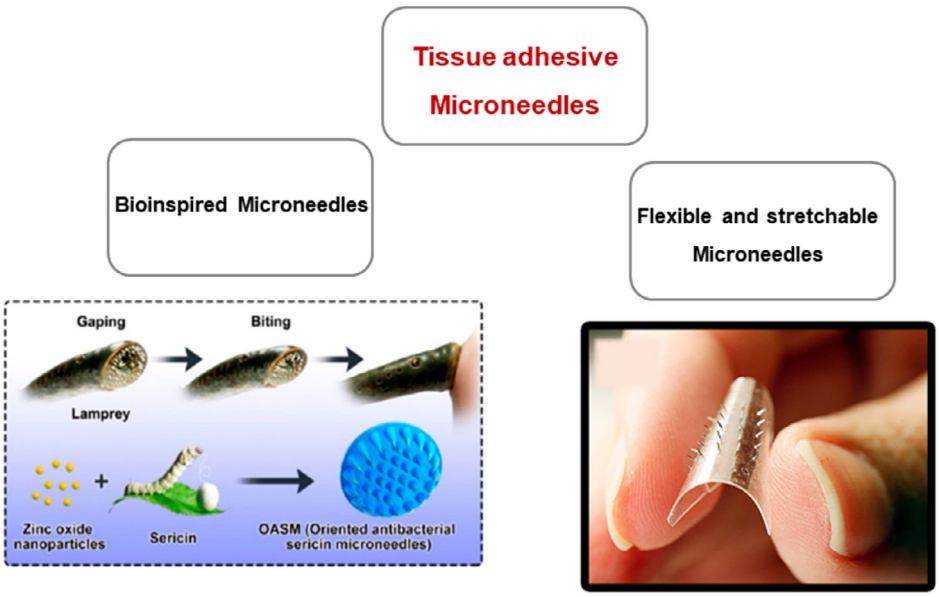

Figure 6. Schematic of topics discussed in the following subsections on design criteria involved in tissue-adhesive microneedles. Reprinted with permission.[102] Copyright 2022, ACS Publications. Reprinted with permission.[106] Copyright 2016, PLOS.

achieve specific desired outcomes.[43] One particular focus is on enhancing the tissue adhesion capability of microneedles. Traditional microneedles face challenges in adhering firmly to tissue surfaces for prolonged periods. However, microneedles with unique bioinspired morphological structures have proven to have better tissue adhesion.[95,96]

Many organisms in nature showcase remarkable adhesion capabilities, often attributed to molecular interactions or microstructures on their surface.[97] Inspired by the barb hangnail structure of porcupine quills, Liu et al. fabricated porcupine quill-like microneedles with a polyacrylamide-polydopamine/Cu2+ (PAM-PDA/Cu2+ (PPC)) composite hydrogel supporting layer.[97] The tissue adhesiveness is achieved through a combination of physical interlock resulting from the multilayer morphology and chemical bonding of the hydrogel patch.

Notably, the applications of microneedles have expanded beyond the skin and exterior body parts, demonstrating great potential for use in internal organs.[98] The tissue adhesiveness property of microneedles has proven equally beneficial for these internal sites. Accordingly, a patch of bioinspired adhesive gemcitabine-loaded gelatin methacryloyl microneedles was designed for pancreatic cancer therapy.[98] Inspired by octopus tentacles, the microneedles on the patch were equipped with a set of suction cups, as shown in **Figure 7**A. These suction cups create a pressure difference that helps the microneedle array adhere to the wet and irregular surface of pancreatic tumor tissue.

In some cases, two techniques, physical locking features and hydrogel swelling, can be integrated into one system to enhance microneedle tissue adhesiveness. For instance, Amer et al. developed a patch of hydrogel microneedles with a self-adhesive barb-shaped interlocking structure for sustained ocular drug delivery.[99] The microneedles feature a locking structure positioned at the waist of each needle. Once inserted into the tissue, the upper section of the needle is fixed into the sclera due to the locking mechanism. Simultaneously, the interlocked part of the microneedle swells due to body fluid absorption by the hydrogel. This swelling creates a strong physical interlock, preventing detachment. This approach significantly enhances tissue adhesiveness, demonstrated by an 80% improvement compared to nonfeatured microneedles. Moreover, the locking feature results in only a slight increase in the required insertion force.

Due to the locking feature of this generation of microneedles, strong tissue interlock might be accompanied by difficulty in microneedle extraction.[100] An increase in the extraction force for patch removal may lead to pain or even tissue damage, which contradicts the original purpose of microneedle applications. Addressing this problem and ensuring the ease of microneedle removal is of interest. To resolve this issue, in continuation of their previous work, Amer et al. developed a patch consisting of smart photoresponsive adhesive hydrogel microneedles.[100] A mixture of polyvinyl alcohol and spiropyran-conjugated N-isopropylacrylamide (NIPPAM) was prepared to make the photoresponsive hydrogel microneedles. Figure 7B shows that the needles underwent swelling and shrinking upon exposure to a light source. By adjusting the concentration of spiropyran conjugated in the hydrogel, the team achieved a 20% reduction in both the width of the locking part and the required microneedle extraction force, providing an efficient strategy to alleviate the difficulty in microneedle extraction.

In addition to their widespread applications as drug delivery or biosensing tools, microneedles with additional therapeutic functions may serve as wound healers.[101] In infected wounds, the natural tissue barrier is often extensively damaged, allowing microorganisms to penetrate subcutaneous layers and leading to a delayed healing process. Moreover, the presence of exudate and necrotic tissues in the wound further complicates the delivery of antibacterial agents, as they cannot easily pass through the tissue layers to reach the deeper locations.[102–104] In such scenarios, microneedles emerge as a suitable solution for delivering therapeutic agents to the deeper layers of the wound. By bypassing the compromised tissue barriers, microneedles can effectively transport therapeutic agents to the affected areas, promoting faster healing and aiding in treating infected wounds.

In an effort to expedite the healing process of linear wounds, Zhang et al. proposed a unique claw-inspired patch of microneedles.[105] This patch comprises two hydrogel microneedle arrays connected by a piece of gauze. Inspired by the clamping structure of the eagle's clawed toes, which enable the bird to grab and hold its prey tightly, the microneedles in this patch were oriented toward each other. This design allows the structure to fix and tighten the wound area, preventing it from secondary dehiscence or reopening.

Similarly, by capitalizing on the wound enclosure strategy for accelerating the healing process, Deng et al. developed a patch containing sericin zinc oxide nanoparticles (NPs)-loaded microneedles with a lamprey teeth-shape distribution pattern.[102] In contrast to conventional microneedle arrays where the needles are uniform and vertically positioned on the patch, the position and size of the microneedles were intentionally varied in this design. The central parts of the patch are covered with shorter needles, while the needles on the round base are longer and oriented at a 30° inward angle, as shown in Figure 7C. This set of structures allowed for the complete binding of skin lesions. The shorter central microneedles were inserted into the wound area, while the longer and tilted-edge microneedles provided a dragging force from the edge of the base substrate toward the center. This stimulation of wound contraction accelerated the healing procedure.

2.3.2. Flexible and Stretchable Adhesive Microneedles

Besides introducing different morphologies to enhance tissue adhesion in microneedle structures, altering the materials used in the microneedle array can also impart this property.

Microneedles with flexible and stretchable backing substrates have the potential to revolutionize how these devices interact with tissue. Using flexible materials for the backing substrate of the microneedle patch, a secure attachment of the microneedle array system to the tissue is achieved. This effectively prevents undesired detachment of the patch throughout the process while also imparting the structure with the remarkable ability to adhere to various body parts.

In practice, most microneedle arrays are commonly prepared as single, solid components. Both needles and supporting substrate are made of the same material. Microneedles must possess mechanical strength and rigidity to prevent breakage and be sharp enough to facilitate easy skin penetration. On the other

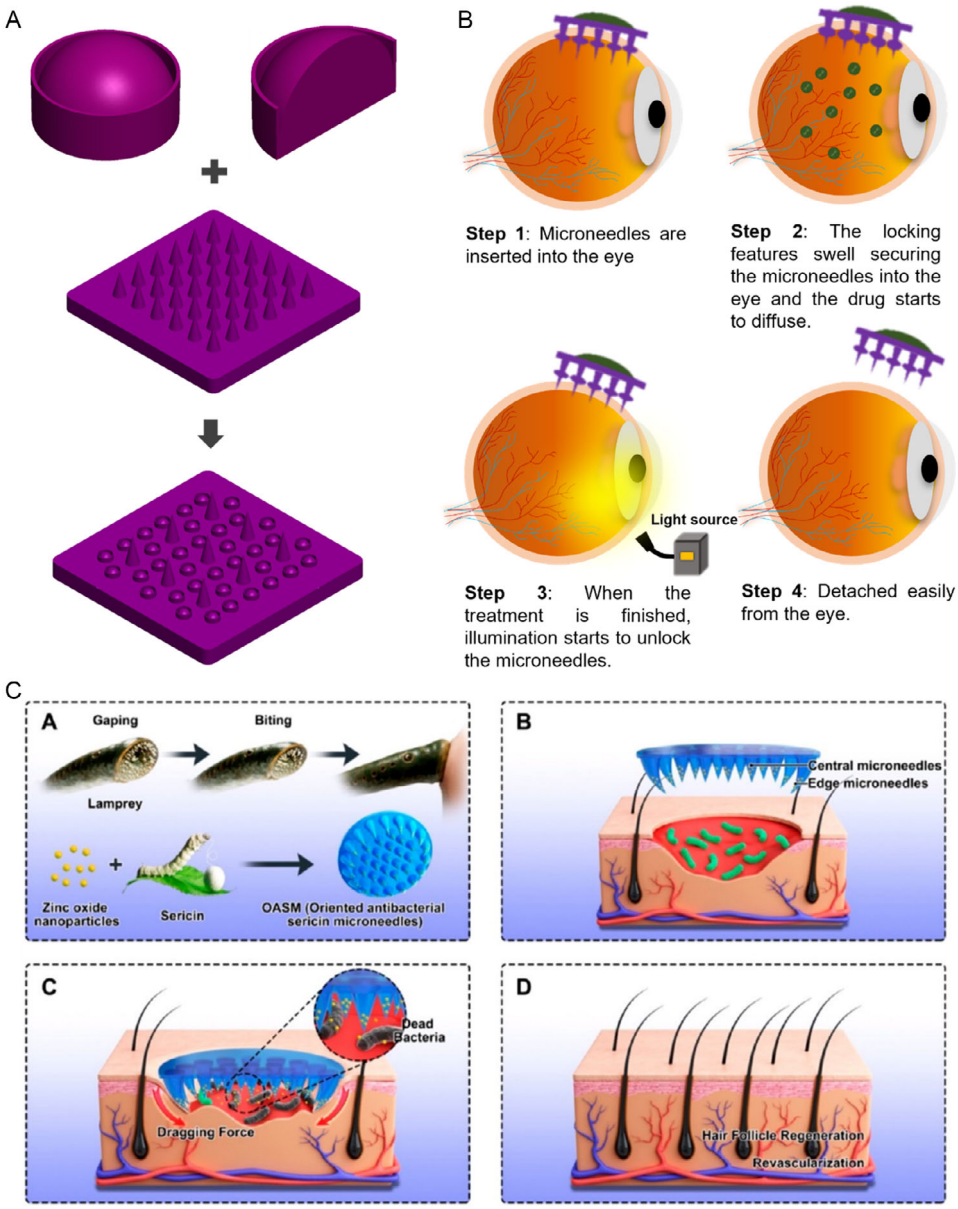

Figure 7. Schematics of A) adhesive gemcitabine-loaded microneedles integrated with octopus-inspired suction cups. Redrawn with some changes from ref. [98], Copyright 2022, Elsevier. B) Insertion and extraction process of photoresponsive adhesive microneedles. Redrawn with some changes from ref. [100], Copyright 2022, ASME. C) (i) Lamprey teeth-inspired oriented antibacterial sericin microneedles. (ii) The needle pattern structure on the patch. The patch consists of two different structures of central short needles with inclined-edged long needles. (iii) Microneedle application process in the infected wound area. Central needles hold the role of releasing NPs to kill the bacteria. The edged needles apply the dragging force to stimulate wound contraction. (iv) The repaired tissue. Reprinted with permission.[102] Copyright 2022, ACS Publications.

hand, the supporting substrate should preferably be flexible to effectively conform to the contours and movements of the tissue.[106] This flexibility reduces the risk of patch detaching from the skin and subsequently enhances wearer comfort. While monolithic polymer microneedle arrays can offer some degree of flexibility in the supporting substrate, there are limitations. Using a soft polymer for the base may adversely affect the mechanical strength and sharpness of the needle tips, potentially making it challenging for microneedles to be reliably inserted into the tissue. Rajabi et al. provided an alternative of two-layered polymer technology, which has the potential to create patches with microneedles made of a rigid polymer in combination with a soft polymer substrate.[106] This approach balances the mechanical properties required for effective skin penetration and wearer comfort.

In this regard, Rajabi et al. implemented a flexible and stretchable patch of microneedles consisting of a flexible base substrate with durable, sharp stainless steel needles.[106] An elastomeric polymer base allows for a seamless fit between the patch and the intricate texture of the underlying tissue. Concurrently,

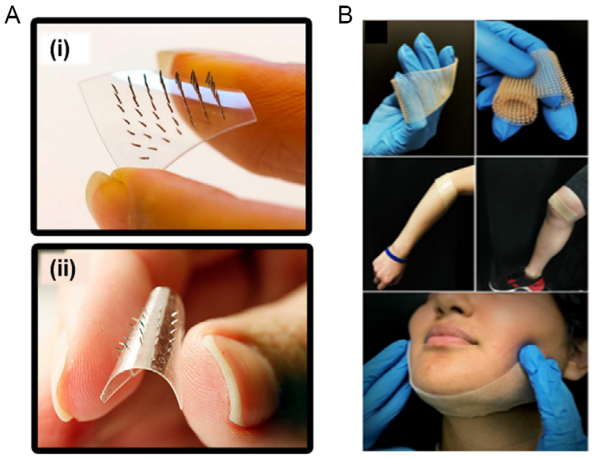

Figure 8. A) Photographs of the microneedles with (i) higher Young's modulus followed by a less flexible backing substrate and (ii) lower Young's modulus and higher flexibility. Reprinted with permission.[106] Copyright 2016, PLOS. B) Photographs of a flexible, stretchable porous microneedle patch. Reprinted with permission.[107] Copyright 2022, Nature.

the robust and sharp stainless-steel microneedles consistently puncture the skin's outer layers. **Figure 8**A shows the fabricated microneedles. The results confirmed the effectiveness of the microneedles in puncturing the tissue and their ability to conform to the skin's wrinkles and deformations.

Sadeqi et al. introduced a polymeric porous microneedle patch fabricated from biocompatible and photocurable resin that can load solid, concentrated drug formulation,[107] as shown in Figure 8B. This study showcased the development of extensive, flexible, and stretchable microneedle patches, covering an impressive surface area of $6 \times 20\,cm^2$, capable of delivering drugs to any body part.

Continuing with a series of studies in this field, a highly flexible and porous silk fibroin (SF) microneedle wrap, referred to as the silk microneedle wrap, was introduced for the direct injection of antiproliferative drugs into the anastomosis sites while ensuring adequate vascular exchanges.[108] The microneedle array was realized by transfer molding of drug-loaded silk microneedles onto a highly flexible and porous silk wrap. The improved cell compatibility, molecular permeability, and flexibility of the silk microneedle wrap play a crucial role in maintaining the structural integrity of blood vessels. The silk wrap effectively supported the silk microneedles, facilitating multiple microneedle penetrations into the target tissue. The study showed a significant inhibition of intimal hyperplasia demonstrated by the silk microneedle wrap over 28 days, leading to a remarkable 62.1% reduction in neointimal formation.

3. Design Considerations

3.1. Mechanical Insertion Performance

In general, for microneedles in therapeutic or biosensing applications, emphasis is placed on their mechanical insertion behavior. Mechanical insertion performance, which encompasses the mechanical stability of the needles and their ability to pierce the tissue and penetrate to the desired tissue depth under applied force, is a key aspect of microneedle development. In this context, microneedles must exhibit sufficient strength to withstand the insertion force necessary to puncture the tissue, typically applied by a thumb-operated applicator. This property is heavily influenced by the microneedle morphological factors and material composition.

The term "insertion force" refers to the force needed to penetrate the dermis layer completely. On the other hand, "puncture force" denotes the maximum force required to pierce the outermost layer of the skin, known as the stratum corneum.[109] Once microneedles come into contact with the skin's surface during insertion, the skin deforms, leading to stress concentration and crack formation. Throughout the penetration process, frictional forces arise between the concave skin surface and the sides of the needles. As the tip of the microneedle pushes and deforms the skin, it generates compressive force within the skin. Skin puncture occurs when this generated stress (von Mises stress) surpasses the skin's elastic modulus, causing a sudden decrease in insertion force and enabling easier penetration into the deeper skin layers.[110]

It is important to note that this insertion force should be carefully controlled within a predefined range to ensure that it neither damages the tissue nor the microneedles throughout the entire process, from tissue puncturing to full insertion.[111]

It has been demonstrated that the mechanical insertion performance of microneedles is heavily influenced by their morphology and material properties.

Figure 9 schematically illustrates the topics discussed in the following subsections on factors affecting microneedles' mechanical insertion performance.

3.1.1. Microneedles' Morphology

Razzaghi et al. studied the effects of the 3D printing tilt angle on the structure of 3D-printed microneedles, aiming to control the required puncture force.[112] **Figure 10**A schematically depicts the fabricated microneedles. The team showed that changing the 3D printer tilt angle could alter the microneedle insertion performance. According to their results, the minimum puncture force could be recorded by a 45° printing tilt angle. The puncture force was reduced by 38% using this tilt angle in comparison to the zero tilt angle.

Following control over the puncture and insertion forces, the inserted microneedle should achieve maximum tissue penetration without contacting nerve vessels in deeper layers. However, due to the inherent properties of body tissues, microneedle insertion faces numerous challenges. The skin may fold around the inserted needle, preventing the complete insertion.[113] The depth to which a microneedle can penetrate the tissue directly affects its efficiency in therapy or sensing. In essence, partial or incomplete insertion can lead to impaired functionality. The significance of achieving the maximum possible penetration depth becomes even more pronounced when dealing with dissolving microneedles. Since the drug

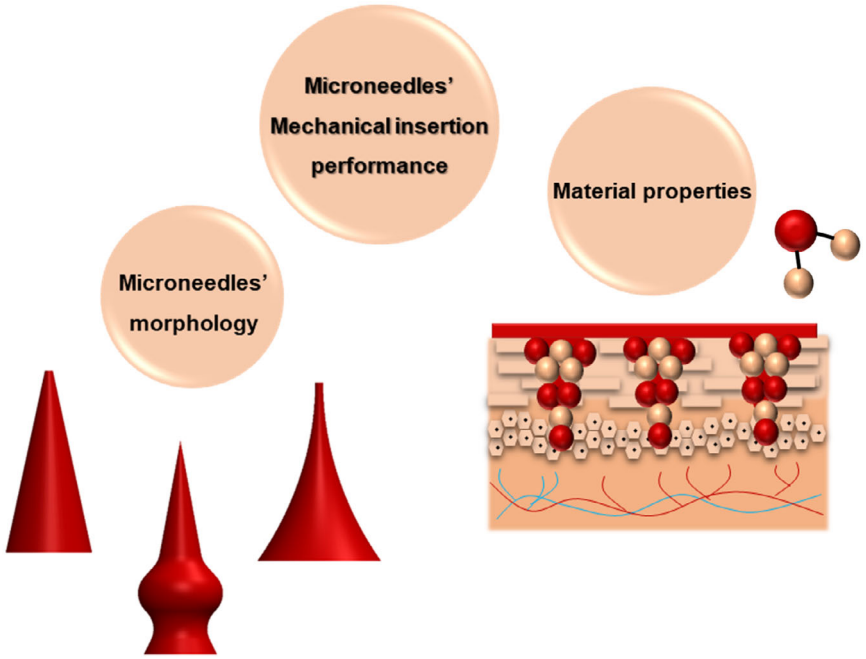

Figure 9. Schematic of the microneedles' morphology was redrawn with some changes from ref. [116], Copyright 2023, Elsevier.

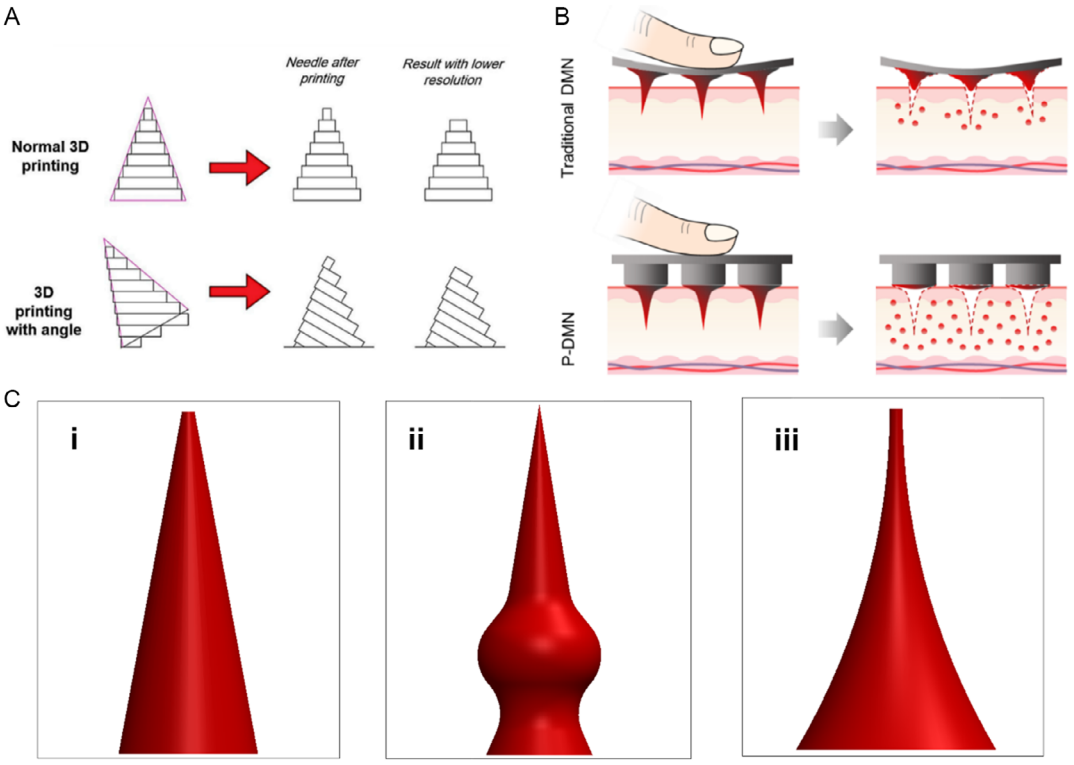

Figure 10. A) Effect of the printing tilt angle on microneedle tip sharpness. Reprinted with permission.[112] Copyright 2023, MDPI. B) Illustration of a micropillar-integrated microneedle patch and its impact on the penetration depth and comparison with a traditional microneedle array. Reprinted with permission.[114] Copyright 2019, MDPI. C) Schematic illustration of (i) conical, (ii) candlelit, and (iii) funnel microneedle structure. Redrawn with some changes from ref. [116], Copyright 2023, Elsevier.

substance is distributed throughout the entire structure of the needles, partial insertion can lead to complete procedure failure.

To address this challenge, in one study, an array of dissolving microneedles integrated with micropillars was prepared to enhance the delivery efficiency of the encapsulated model drug by improving microneedle penetrability compared to traditional designs,[114] as shown in Figure 10B. In this structure, dissolving microneedles were positioned atop the micropillars. The design ensured that only the dissolvable segment, rather than the pillars themselves, was inserted into the tissue layers. The pillars effectively served as enhancers, facilitating the full insertion of dissolving microneedles. The results demonstrated a significant enhancement in the delivery efficiency of the encapsulated drug using micropillar integrated dissolving microneedles (P-DMN) compared to the traditional design. The drug delivery efficiency was $91.83\% \pm 7.75\%$ for these fabricated microneedle structures, compared to $64.86\% \pm 8.17\%$ for conventional dissolving microneedles. Furthermore, the skin penetration accuracy rate for P-DMN was $97.78\% \pm 2.22\%$, evidencing its superiority over the conventional style, which had an accuracy rate of $44.44\% \pm 7.85\%$.

It is well known that gradual volume reduction of microneedles from the base to the tip is essential for achieving sharp needles capable of successfully piercing tissue. However, this asymmetry in their shape on the z-axis poses challenges for efficient drug release. In case of partial insertion, a significant portion of the therapeutic compound may be missed. Under such circumstances, one solution is to relocate the drug container within the lower sections of the needles, closer to the tips.[115] This approach increases the drug-carrying capacity of the needles in the area more likely to be inserted, improving the chances of effective drug delivery.

As a trial, Min et al. addressed the issue of drug capacity distribution within microneedles by fabricating various dissolving microneedle shapes, including conical, candlelit, and funnel shapes,[116] as shown in Figure 10C. These shapes were assessed for their performance in terms of penetrability and drug delivery efficiency. The conical needle structure was designed with a linear change in radius from base to tip. The candlelit-shaped dissolving microneedle featured two inflection points at its widest sections, leading to a varied drug capacity distribution throughout the needle's volume. The distribution decreased from the tip to the first inflection point and then increased again toward the second point. In contrast, the funnel-shaped needle exhibited an exponential change in radius from base to tip, providing a higher drug-carrying capacity at the bottom of the structure compared to the conical shape.

The results showed that the needle's shape significantly influenced the depth of microneedle penetration and drug delivery efficiency. For the conical, candlelit, and funnel-shaped microneedles, the volume inserted during insertion was 48.0%, 69.8%, and 10.2%, respectively, followed by 58%, 75.4%, and 16.3% of the total volume dissolved during the insertion process. These findings proved that the candlelit structure is the most efficient model among the three shapes, which could achieve the largest penetration depth and more effective drug release behavior.

3.1.2. Microneedle Material Properties

In addition to the role played by microneedle morphology in determining the mechanical behavior of the structure, material composition also affects performance in terms of required insertion force, mechanical strength, and penetration depth. Microneedles can be flexibly fabricated from a variety of materials, including metals and organic compounds.[117] The effort to achieve a structure with satisfactory strength under insertion force is one of the leading motivations behind offering such a wide range of material selections.

Metals have proven to be among the toughest and most resistant to applied force. However, the potential severity of accidental needle breakage in tissue, such as irritation and inflammation, necessitates their substitution with biocompatible polymers. To ensure mechanical strength, polymers often require refinement, typically achieved by synthesizing two or more polymers in variable ratios.

For instance, in a study conducted by Machekposhti et al. a patch of biocompatible polymeric microneedles was fabricated for tranexamic acid delivery.[118] The patch was made from two different types of polymers: polyvinylpyrrolidone (PVP) and methacrylic acid (MAA) in various PVP/MAA ratios (100/0, 95/5, 90/10, 85/15, 80/20). Based on their findings, the PVP/MAA (90/10) ratio provided the best performance in terms of mechanical resistance of the prepared needles.

In another study, Bonfante et al. demonstrated the effects of different materials on microneedle mechanical strength and tissue-piercing capability.[119] In this regard, three sets of microneedles fabricated from carboxymethyl cellulose (CMC), alginate, and hyaluronic acid (HA) were analyzed in terms of geometrical parameters, piercing ability, and dissolution rate. The concentration of materials in deionized water ranged from 1 to 5% (w/w) to ensure quick microneedle dissolution and stability upon tissue insertion. Each material yielded microneedle arrays with different geometrical parameters. All fabricated samples failed the tissue piercing test at a concentration of 1% (w/w). Based on the piercing test results, HA at a concentration of 3% (w/w) successfully pierced aluminum foil. Only 87.5% of the arrays made from the other two materials, CMC at 5% (w/w) and alginate at 3% (w/w), were able to pierce the foil.

4. Fabrication Methods

4.1. Molding Techniques

Micromolding, as a microneedle fabrication method, involves a series of stages to replicate microneedle structures using prefabricated molds. This method has been widely employed in microneedle fabrication. The typical process involves multiple steps of solvent casting or polymerization into a female mold structure. The female mold can be fabricated with lithography or laser machining.[120]

Zhang et al. employed the layer-by-layer replication molding technique to manufacture a patch composed of multilayer pagoda-like microneedles.[121] **Figure 11**A schematically illustrates the fabrication procedure. Initially, a prepolymer solution was introduced into a negative mold containing conical holes.

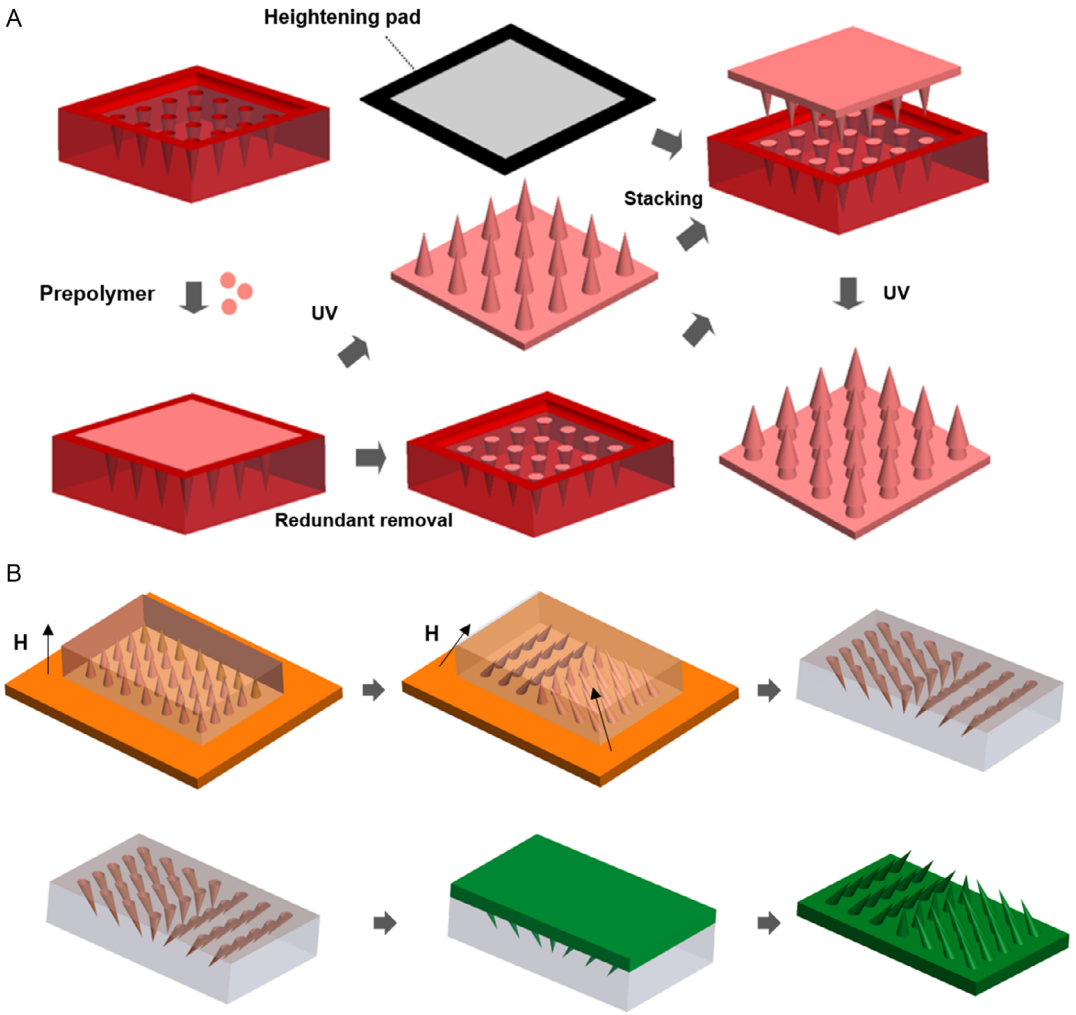

Figure 11. A) Schematic of multilayer pagoda-like microneedles fabricated using layer-by-layer replication molding technique. Redrawn with some changes from ref. [121], Copyright 2021, Elsevier. B) The fabrication process of praying mantises' forelegs-inspired microneedle array using the ferrofluid-based molding technique. H represents the direction of the applied magnetic field. Redrawn with some changes from ref. [122], Copyright 2019, Elsevier.

This solution was then solidified by ultraviolet light (UV) to create a precursor microneedle patch. The precursor patch was detached from the mold, and then the negative mold was refilled with the prepolymer solution. After removing the excess solution, a half-filled negative mold was generated. This mold was combined with a hollow heightening pad and the previously prepared precursor patch, stacking them from bottom to top. The stacked structure was exposed to UV irradiation, binding the second layer to the precursor patch, resulting in a double-layer microneedle patch. The interlayer spacing could be adjusted by varying the thickness of the heightening pad. This method was shown to be applicable for fabricating microneedles with more than two layers, including triple-layer and tetralayer microneedle patches. The boundaries between layers were distinct, and the interlayer spacing remained uniform even with an increasing number of layers.

The ferrofluid-based molding technique is particularly suitable for producing microneedle arrays with inclined and asymmetric needle patterns, in contrast to the conventional micromolding approach, which is more suited for upright and symmetrical needle structures.[122] In the ferrofluid-based molding technique, ferrofluids containing ferromagnetic NPs are dispersed into small conical droplets. These droplets can be manipulated using an external magnetic field to create magnetically oriented patterns. By applying and controlling the magnetic force, these conical droplets start to rotate and tilt, ultimately forming asymmetrical arrays. This technique offers a versatile approach for fabricating microneedle arrays with non-traditional shapes and orientations.

The ferrofluid-based molding technique, inspired by the microstructures found on praying mantises' forelegs, generated a patch of microneedles with inclined clamping needle structures.[122] The fabrication process involved ferrofluids within a nonmagnetizable ultraviolet (UV) curing prepolymer mixture, as shown in Figure 11B. A cylindrical magnet positioned beneath the structure induced magnetic hydrodynamic instability,

causing the ferrofluids to fragment into distinct conical droplets. When the external magnet was rotated from its initial longitudinal alignment toward a transverse orientation, the ferrofluid droplets aligned with the tilted magnetic induction lines, adopting a slanted configuration. The angle of magnet rotation influenced the inclination angle and dimensions of the main structure. By adjusting the external magnetic force or changing the distance between the substrate and the magnet, the configuration and size of the microneedles could be altered. To address the issue of microneedle collapse after drying, poly-(ethylene glycol) diacrylate (PEGDA) was added to increase stability.

4.2. Laser Micromachining

Laser micromachining stands out as a flexible and versatile method for fabricating microneedles. This technique operates independently of a clean room facility, making it convenient to produce microneedles with diverse morphologies and materials quickly. Laser micromachining emerges as a promising strategy because it can easily, precisely, and rapidly generate microneedles with complex geometries. The customization of microneedle size and shape relies entirely on specific laser parameters such as laser power, frequency, and speed.[123]

Guo et al. fabricated a shark tooth-inspired microneedle dressing for intelligent wound management using the laser engraving.[124] Aiming to increase the patch's tissue adhesiveness for efficient wound healing purposes, the needles were designed in flat and inclined patterns, as shown in **Figure 12**B. Due to its flexibility, polyurethane (PU) was chosen for the base substrate of the microneedle patch. First, the PDMS mold was pre-stretched to specific ratios and tilted at different angles, as shown in Figure 12A. Subsequently, arranged patterns of microneedles were engraved onto the molds. Following the restoration of the molds to their initial conditions, a solution containing SF precursors was introduced into the negative mold using drop casting. Any trapped air was removed through degassing cycles. The negative mold containing the SF precursor solution was positioned at room temperature to make needle tips composed of SF. Subsequent treatment with 90% methanol for 10 min was performed, after which a solution of PU-SF precursors was deposited into the mold using drop casting. The solution was then dried, leading to the formation of a flexible base. Finally, the prepared microneedle patch was carefully detached from the mold. The SF-based needle tips conferred impressive mechanical robustness to the microneedle patch, while the PU base granted the patch flexibility.

Taking inspiration from the intricate folding patterns found in insect wings, Wang et al. introduced a 3D origami microneedle patch,[125] as shown in Figure 12C. This patch possesses multiple functions, including detecting biomarkers, controlling the release of drugs, and sensing motion, toward smart wound management. A laser engraving machine carved out a finely detailed needle structure onto a stretched negative mold made of Ecoflex

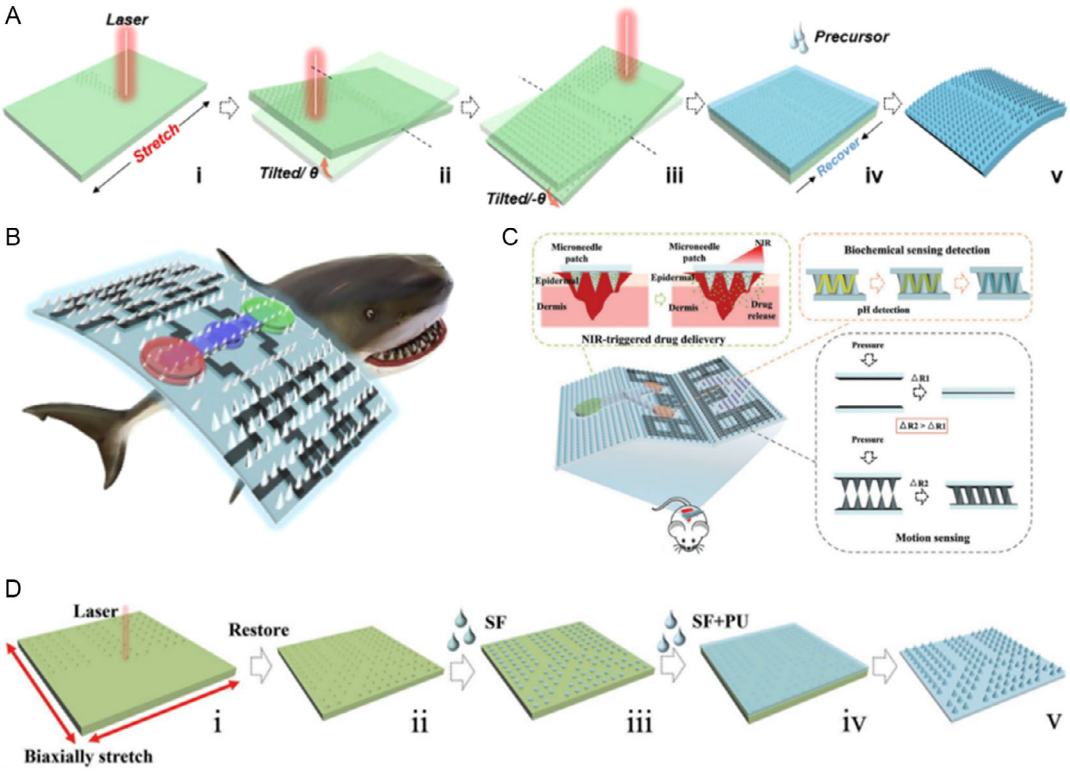

Figure 12. A) Schematic illustration of shark tooth-inspired microneedle array. Reprinted with permission.[124] Copyright 2021, ACS Publications. B) The structure of the shark tooth-inspired microneedle wound dressing for intelligent wound management. Reprinted with permission.[124] Copyright 2021, ACS Publications. C) View of the insect wings-inspired 3D origami microneedle patch. Reprinted with permission.[125] Copyright 2023, Wiley VCH. D) Fabrication process of the origami microneedles. Reprinted with permission.[125] Copyright 2023, Wiley VCH.

material, as shown in Figure 12D. To create the microneedle patch consisting of SF and a polyurethane (PU) biphasic material, the SF solution was initially poured into the mold's cavities and subjected to vacuum drying multiple times to remove air. Excess SF solution was eliminated, and the SF solution within the cavities was air dried at room temperature, resulting in arrays of SF-based microneedles. Following this, a mixture of SF and PU was poured onto the mold, deaerated using a vacuum dryer, and subsequently heated and cured. This process resulted in producing the final SF-based biphasic microneedle patch, which was then removed from the mold.

4.3. Printing Method

4.3.1. 3D Printing

3D printing encompasses a diverse range of additive manufacturing techniques, wherein materials are added layer by layer in a controlled manner to prototype a 3D model.[126] In terms of resolution, 3D printing can be classified into fused deposition modeling (FDM), stereolithography (SLA), digital light projection, jet printing, and two-photon polymerization (2PP), which are among the most common fabrication approaches for microneedles.

Some of the present 3D printing fabrication methods, such as FDM, inkjet printing, and selective laser sintering, need postprocessing, as intended detailed morphology could not be well achieved. However, sometimes, it is difficult to completely manage the degree of the postprocessing procedure and control the microfeatures.[127] 2PP holds the best resolution in fabricating even submicrometer needles among these methods. 2PP, also known as laser direct writing, has demonstrated an excellent capability in fabricating sharper microneedles compared to other 3D manufacturing techniques. A femtosecond or picosecond laser is usually employed in this approach. The polymerization process is initiated through the absorption of two photons (TPA) upon exposure to a concentrated laser pulse. This results in a unique energy pattern centered on the laser's focal point, directed at the light-sensitive photoinitiator molecules to start the polymerization process. They absorb this energy within specific regions called "polymerization voxels". These voxels are areas where the absorption energy surpasses a defined threshold of the resin, creating a 3D micro-/nanostructure through polymerization.[128]

A patch consisting of pyramidal microneedles whose lateral sides were decorated with designs inspired by European true bugs' external scent efferent array structure for unidirectional drug transport from the bottom toward the tip of the needle was fabricated using 2PP.[25] A laser beam with a wavelength of 515 nm, pulsing at 1 MHz with a pulse duration of 290 fs, was concentrated into the photoresist using a magnifying lens with 50′ magnification and a numerical aperture of 0.42. The process creates microneedles in layer-by-layer format, each with a thickness of 1 μm, within a sandwich sample arrangement.

Szeto et al. presented a patch of 2PP 3D-printed ultrasharp hollow microneedles for aspiration of microliter volumes of perilymph from guinea pigs for proteomic analysis.[129] The team demonstrated that these microneedles facilitated aspiration of perilymph across the round window membrane without lasting anatomic damage to it and no significant functional consequences on hearing. The needle's inner channel, which had a circular cross section, was deliberately designed to vary in its cross-sectional area along the needle's length (**Figure 13**A). This channel extends throughout the needle shaft, and the shaft's outer diameter constrains its dimensions. The channel widens at the base of the needle where the outer diameter is larger, reducing the fluidic resistance. This is significant as fluidic resistance decreases inversely with the fourth order of the diameter. Toward the needle's tip, the channel curves from the shaft's center and opens to the side of the microneedle. This design choice enhances the bending stiffness by keeping the hollow section close to the central axis while preserving the tip's geometry. Employing additive manufacturing techniques facilitated the realization of these features, which could be challenging to achieve with traditional methods. SLA files were generated and processed using the Describe software with a slicing distance of 1 μm and laser intensity of 80%. The fabrication of microneedles was performed using the 2PP technique. Subsequently, the microneedle was affixed to a 2-inch-long, 30-gauge, blunt small hub-removable needle using epoxy glue and sterilized using ethylene oxide gas.

When employing a 3D printing fabrication approach, achieving microneedles with satisfactory mechanical performance poses a significant challenge. In general, regardless of the specific fabrication technique, certain criteria must be met, especially when dealing with intricate microfeatures. The chosen printing strategy should be capable of effectively manufacturing delicate micrometer-scale devices. Moreover, apart from the microneedle's geometry, the selected printing method can also influence the mechanical performance.[127] Although the 2PP printing technique has demonstrated impressive capabilities in creating microneedles with highly detailed micrometer-scale features, concerns have arisen regarding its potential to deliver mechanically robust needle structures.

According to the abovementioned concern, Li et al. utilized magnetic field-assisted 3D printing (MF-3DP) to fabricate limpet teeth-inspired microneedles.[127] Figure 13B shows the sequence of the microneedle fabrication process. Microneedles were manufactured using a combination of reinforced iron oxide particles (IO) as nanofillers. Using the MF-3DP technique, these microneedles were constructed using aligned iron oxide NPs (aIOs) within a polymer matrix. The MF-3DP process successfully replicated the hierarchical structures found in limpet teeth, resulting in exceptionally robust microneedles. The method achieved precise alignment of microfillers under magnetic guidance. By crosslinking the photocurable polymer selectively, the MF-3DP process encapsulated the aligned NP bundles within the printed microneedles. The 3D-printed hierarchical design with aIOs exhibited improved mechanical properties compared to those with randomly positioned iron oxide NPs (rIOs). The limpet tooth-inspired architecture improved mechanical strength by aligning IOs in each layer.

4.3.2. 4D Printing

The 3D printing method seems to be the best solution for fabricating microneedles with complex geometry among all the existing fabrication methods. However, in more complex

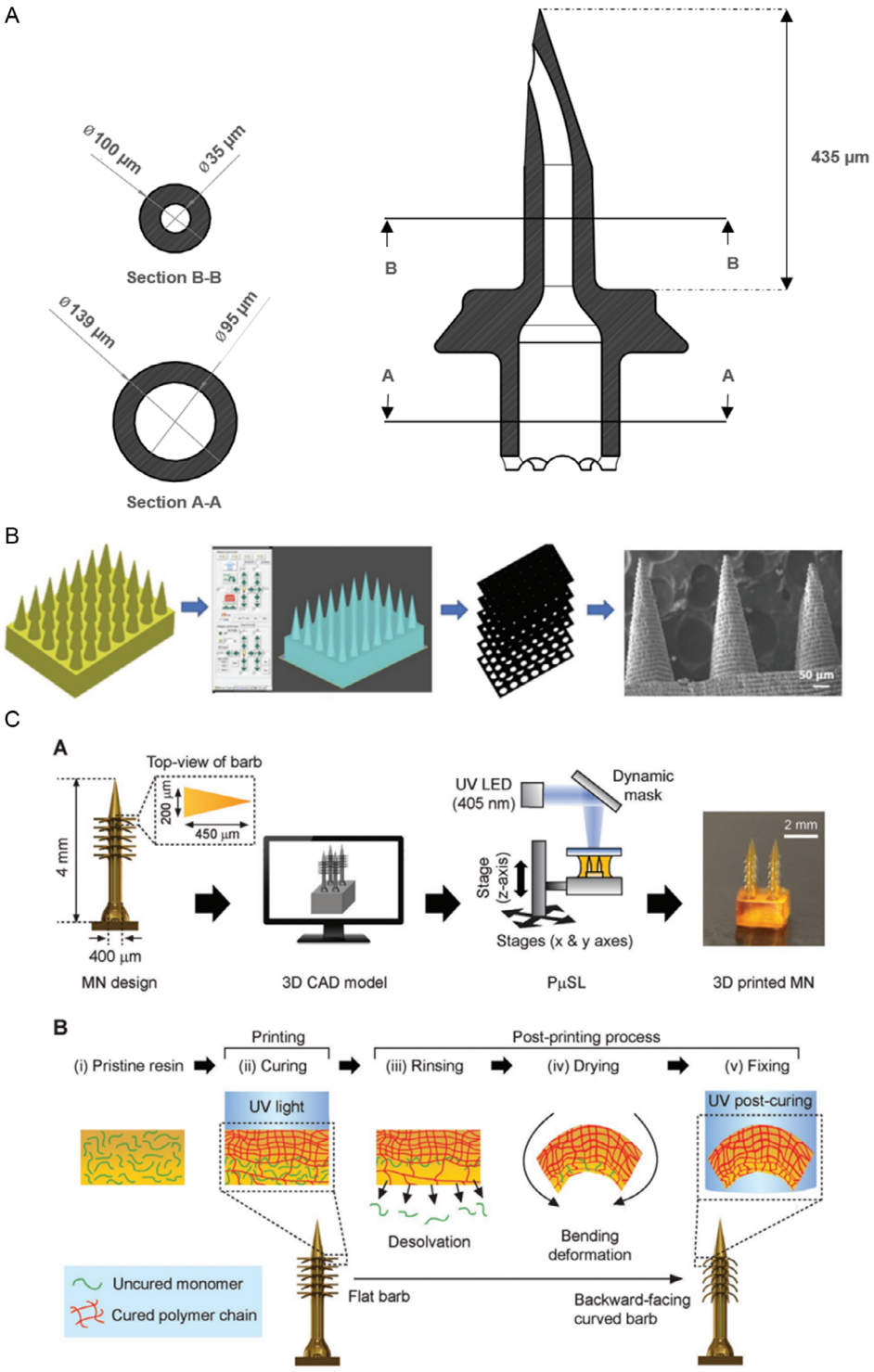

Figure 13. A) Cross-section view of 2PP 3D-printed hollow microneedle for perilymph sampling application. Redrawn with some change from ref. [129], Copyright 2021, Elsevier. B) Schematic view of the fabrication process of microneedles using MF-3DP technique. Reprinted with permission.[127] Copyright 2021, Wiley. C) 4D printing procedure for formation of the horizontally structured barbs into backward-facing design. Reprinted with permission.[130] Copyright 2020, Wiley.

cases, such as structures with protrusions on the surface of the needles, the 3D printing method may not be applicable. This is where the 4D printing approach can demonstrate a better performance compared to 3D printing. The 4D printing method is defined as a 3D printing platform in which smart stimuli-responsive materials are used. Stimuli-responsive materials

would allow for a more complex morphology. These materials are sensitive to external stimuli. Once the structures are exposed to these stimuli, their response includes elongation, bending, twisting, or a combination of these deformations. These postprinting procedures result in programmed shape deformations.[130]

Han et al. fabricated a patch consisting of bioinspired microneedles with backward-facing curved barbs using 4D printing to enhance the microneedles' tissue adhesion.[130] This method relies on a digital light processing 3D microprinting technique called projection micro-SLA (PμSL) and the deliberate deformation of barbs during the printing process through the manipulation of crosslinking density gradients. The shaft of the microneedle was designed with a conical shape. Triangular barbs were positioned on the outer surface of the microneedles. The fabrication of the 3D microneedle array was achieved using PμSL, where a 3D model of the array was digitally created, sliced into cross-sectional images, and then patterned light (405 nm) was projected onto a photocurable precursor solution, Figure 13C. This process is repeated layer by layer, constructing the 3D microneedle array. Two additional moving stages were incorporated on the printing plane for larger microneedle arrays for a step-and-repeat process. Furthermore, the high resolution offered by PμSL allowed for further scaling down of microneedle dimensions. Photocurable biocompatible polymers were employed for microneedle fabrication. The barbs must be positioned opposite the needles' tip to realize the microneedle tissue adhesion upon insertion. However, achieving this complex geometry through 3D printing could be challenging due to the layer-by-layer nature of the process, which restricts unsupported structures. Using supporting structures is not feasible in microscale 3D printing due to limitations in multimaterial 3D printing capabilities and sacrificial printable materials. In fact, the 4D printing approach involved horizontally printing the barbs during the initial stages, with photopolymerization initiating at the surface of the precursor solution and gradually propagating inward due to diminishing light intensity, Figure 9C. This results in a gradient of crosslinking density within each layer, with the top part being highly crosslinked and the bottom part having lower crosslinking density. Consequently, some monomers in the bottom portion remained uncrosslinked. After printing, when the microneedle array was rinsed in ethanol, the uncured monomers in the lower part of the barbs diffused out, creating voids in the network. As a result, the lower portion of the barb contracted during the drying process, causing the barb to curve downward. This curved barb shape was then fixed through postcuring via flood UV exposure.

4.4. Hot Embossing

Hot embossing involves transferring a pattern onto a melted polymeric material by heating the polymer up to its glass transition temperature, causing it to soften and become moldable for replication of the desired pattern.[131] The master mold used for creating micropatterns on the polymer can be fabricated using various methods such as laser machining, lithography, micromilling, etc.[131] One of the most notable advantages of this technique is its potential for economically viable mass production.[131] This method has been demonstrated as one of the potential microneedle fabrication methods.

A gradient porous microneedle array (GPMA) was fabricated using a modified hot embossing method under the coupling effects of gradient thermal and pressure multifields.[132] **Figure 14**A schematically illustrates the hot embossing fabrication setup. The pores on the microneedles were in a gradient format, predominantly distributed in the tip section of the needles. The porosity of the generated microneedle structure was 20.1%. The following steps were taken to fabricate the PLGA porous microneedle array structure: The stamp cavity array mold was fabricated on a 2 mm-thick aluminum sheet using a laser micromachining method. The fabricated mold was ultrasonically cleaned for 1 h to prepare it for the next stage. The two blocks located at top and bottom positions were heated to 65 and 50 °C, respectively. The laser-machined cavity array mold was set on the bottom heating block. Then, PLGA powder was uniformly poured into the microcavity structures. The top heating block was slowly lowered and compressed the bottom part with an 800 N insertion force for about 30 min. After this stage, the prepared cavity array mold was removed and cooled to 35 °C for

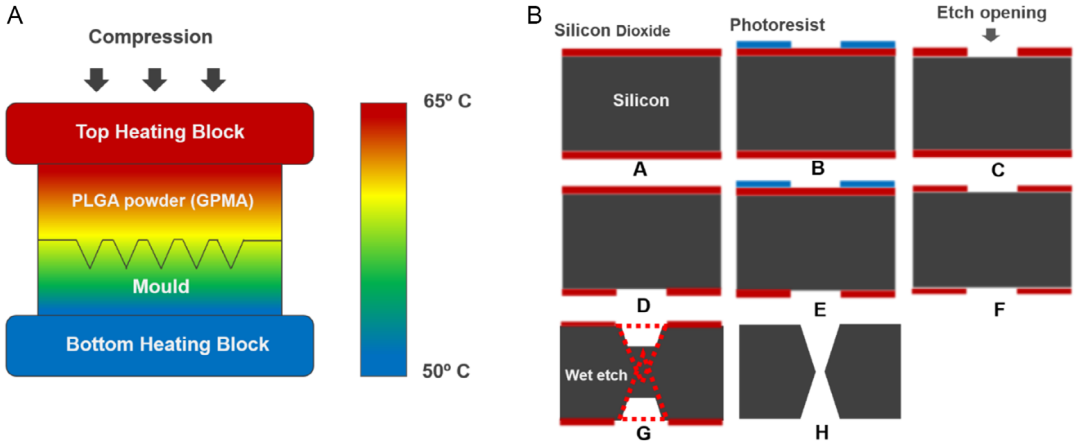

Figure 14. A) Schematic illustration of hot embossing fabrication setup for preparation of GPMA. Redrawn with some change from ref. [132], Copyright 2019, Elsevier. B) Schematic of the fabrication procedure (photolithography + etching) of in-plane silicon pyramidal microneedle array. Redrawn with some change from ref. [135], Copyright 2022, Elsevier.

5 min. The GPMA was peeled off from the cavity mold. Finally, the plasma treatment was conducted on the prepared GPMA.

4.5. Photolithography and Etching

Photolithography followed by etching has been recognized as a microneedle fabrication method since 1998 when the first patch of silicon microneedles was introduced.[133] Photolithography, defined as the process involving ultraviolet (UV) light and X-rays to transfer a pattern onto photoresist polymers, is one of the traditional microneedle fabrication processes. For silicon microneedles, photolithography is followed by etching to remove the unwanted parts of the microneedle structure.[134] A major challenge with this technique is the difficulty in fabricating complex microneedle geometries due to the hard control over the direction and rate of the etching process.

Howells et al. developed a patch of in-plane silicon pyramidal microneedles with a 54.7° side-wall etched angle.[135] Figure 14B schematically illustrates the fabrication procedure. For the fabrication of this structure, both sides of a silicon wafer were initially coated with silicon dioxide (stage A). Photolithography was then used to transfer the pattern onto the surface of the silicon dioxide-coated silicon wafer (stage B). The sample underwent etching into the silicon dioxide hard mask (stage C). The entire photolithography and etching process was repeated for the backside of the silicon wafer (stages D–F). The sample was then submerged into a KOH solution, which simultaneously etched both sides of the silicon wafer, resulting in the generation of V-shaped grooves that intersect to create a pyramidal microneedle structure (stages G and H). Furthermore, this method was used to fabricate hollow microneedles by bonding two grooved microneedles to form an enclosed hollow microchannel. According to their reports, this method demonstrated the potential for fabricating various microneedle array structures with different geometries.

To broaden readers' perspective on this concept, **Table 1** summarizes the key characteristics of the relevant studies in this area.

Table 1. Summary of the research studies in this area.

Microneedle design		Application	Fabrication method	Significance
Core–shell microneedle patch[138]		Vaccine delivery	Micromolding method	Preprogrammed burst release of vaccine payloads over a long period of time through one single administration
Porous metal-organic framework microneedle patch[139]	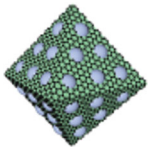	Wound healing	Template replication molding	High drug-carrying capacity due to the microneedle's porosity, controlled drug release.
Mushroom-inspired imprintable and lightly detachable microneedles[140]	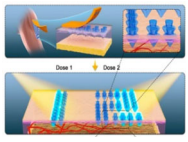	Multidose COVID 19 Vaccine delivery	Micromolding method	Detachable structure from the backing substrate, ability of recording vaccine counts with no need of extra storage, convenient readout.
Bee sting-inspired inflammation-responsive microneedles[141]	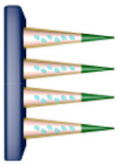	Drug delivery	Micromolding method	Separable needle tips for drug delivery to gingival sulcus with no disruption on normal oral functionality
Octopus-inspired adhesive microneedles[142]	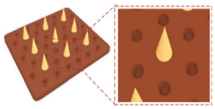	Tissue adhesion and Drug delivery	Diffraction ultraviolet (UV) light lithography	Firm tissue adhesion in wet, dry, and moist environments
Ice microneedles[143]	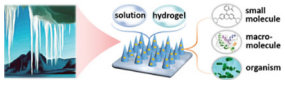	Drug delivery	Freezing template-based method	Efficient penetration. Ability to deliver various types of drug formulations.
Microneedles with different base shapes (circle, triangular, square and star)[144]	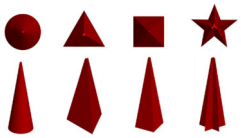	Drug delivery	Micromolding method	Providing efficient skin penetration subsequently effective drug release

Table 1. Continued.

Microneedle design		Application	Fabrication method	Significance
Bioinspired adaptable indwelling microneedles[145]	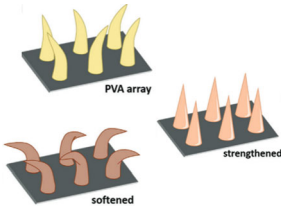	Wound healing	Template replication and 3D transfer printing	Ion-responsive mechanical strength of the microneedles' tips. Tips undergo hardening mode to ensure tissue penetration, then soften once detached from the supporting substrate to adapt the surrounding tissue.
Faceted microneedle array[146]	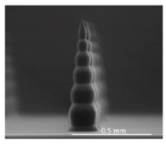	Vaccine delivery	Continuous liquid interface production 3D printing	Large, exposed surface area. Ability to coload multiple vaccine components
Tunable merged-tip microneedles[147]		Drug delivery	Photolithography, elastocapillary-driven self-assembly process	Simple, flexible fabrication method. Customizable and modular platform, capable of adapting a range of design requirements, ensuring it meets specific functional demands.
Microneedle ion sensor-based wearable system[148]	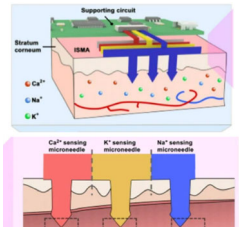	Biosensing	Laser cutting	Three parallel planer microneedle sheets, each is responsible for detecting one specific ion. Capable in simultaneous multiple ions detection.

Redrawn with some changes.[138] Copyright 2021, Nature. Reproduced with permission.[139] Copyright 2022, Wiley VCH. Reproduced with permission.[140] Copyright 2022, ACS Publications. Reproduced under terms of the CC-BY license.[141] Copyright 2023, AAAS. Reproduced under terms of the CC-BY license[142] Copyright 2020, AAAS. Reproduced with permission.[143] Copyright 2021, Wiley VCH. Redrawn with some changes.[144] Copyright 2022, Elsevier. Reproduced with permission.[145] Copyright 2023, Wiley. Reproduced with permission.[146] Copyright 2021, National Academy of Sciences. Reproduced with permission.[147] Copyright 2018, Nature. Reproduced with permission.[148] Copyright 2023, Nature.

5. Grand Challenges and Future Perspective

Several key steps must be meticulously taken from inception to completion of the development process to bring microneedles to real-world applications. The algorithm for microneedle development process, spanning from the outset to the final stages, is visually outlined in **Figure 15**.

The initial step involves specifying the application of microneedles, whether for therapeutic/diagnostic or tissue-adhesive purposes. Subsequently, the overall morphological structure and physical properties of microneedles must be thoughtfully selected to serve the intended use. The selected design should ideally encompass all the relevant aspects of an ideal microneedle structure, although achieving this can sometimes be quite challenging. There are instances where emphasizing one factor may compromise other associated features. For example, in the case of tissue-adhesive microneedles with locking morphological features, it is crucial to strike a balance between the strong adhesiveness of the microneedles and the ease of removing them from the tissue.[136] In most cases, microneedles are designed to adhere to the tissue firmly, but not enough attention has been given to their comfort during removal. It is worth noting that difficulty in removing the patch from the skin can lead to microneedle and/or tissue damage. To address the issue raised by the interlocking part, developing size-tunable microneedles fabricated from smart, stimuli-responsive materials could provide a solution. However, the reliance of the technique on additional equipment could add to the complexity of the procedure. As discussed, using flexible materials for the back substrate of the patch is another viable option for creating adhesive microneedle array systems. This approach could resolve the issue by providing seamless attachment to the tissue without concerns about detachment. It is crucial to carefully consider material selection for these microneedle array systems, as these structures will be used on humans. Potential irritation, inflammation, and toxicity risks must be minimized to prevent exacerbating patient discomfort. Since these needles are applied to various organs and body parts, thorough tests and risk assessments are necessary to ensure material safety and efficacy.

The selection of the appropriate fabrication strategy follows the step of specifying the microneedle design structure. The method chosen for preparing the desired structure must possess

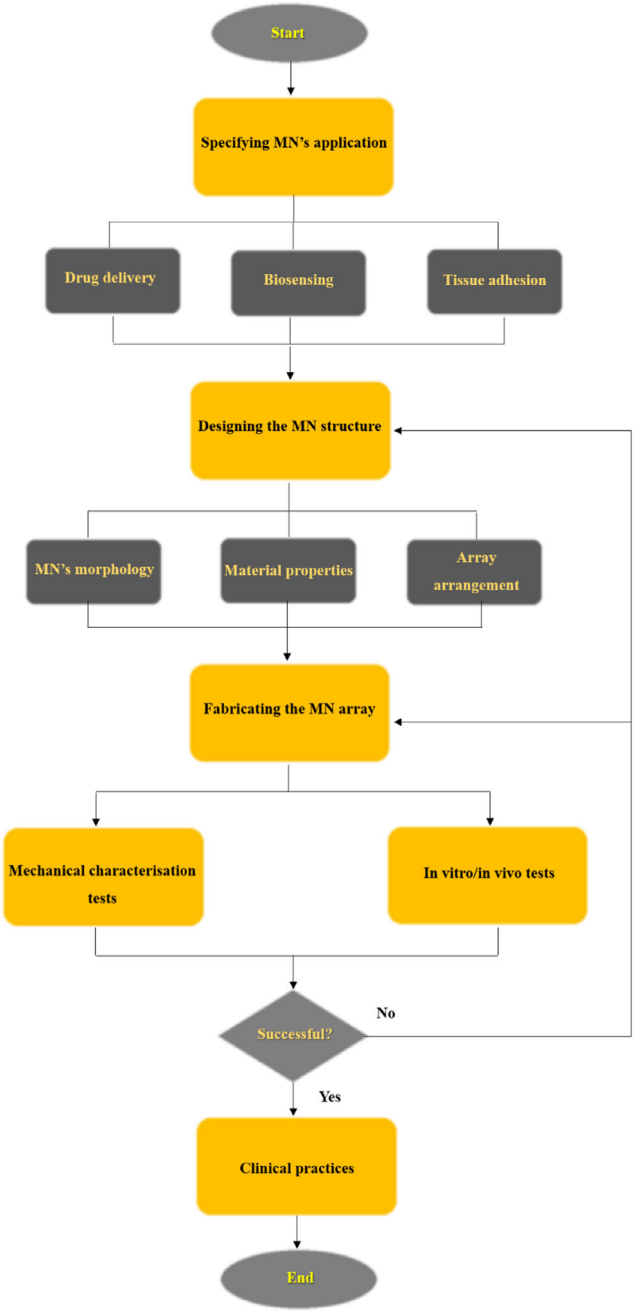

Figure 15. Flowchart of the microneedle preparation sequence.

specific features. Careful consideration is required for factors such as feasibility, flexibility, and cost associated with the chosen method, highlighting the importance of these aspects in decision-making. It is worth noting that, at times, these features may not all be simultaneously attainable. For instance, 3D printing represents a promising approach for manufacturing intricate microneedle structures efficiently in a single-step operation, potentially offering time and resource savings compared to traditional methods.[126] However, its adoption as a preferred preparation strategy is hindered by several limitations. One notable drawback is its limited compatibility with materials beyond resins, which can compromise performance outcomes. Reports have also underscored challenges in achieving mechanically robust microneedle designs through 3D printing, raising concerns about structural durability.

Moreover, the complexity of these structures can significantly extend processing times, rendering 3D printing less suitable for large-scale production. As the move toward mass production of microneedles gains speed for real-world applications, the choice of preparation method emerges as a critical determinant in advancing from laboratory research to clinical implementation. Designers must carefully weigh these considerations to align methodological choices with the primary objectives of microneedle development.

Once the structure is fabricated, if it fails to pass the evaluation tests, that is., mechanical characterization and in vitro/in vivo tests, the process must revert to the initial stage for verification, whether that involves re-evaluating the fabrication process or reconsidering the chosen microneedle design structure.

Following years of dedicated research on microneedles and their laboratory-based fabrication, the current juncture appears to be the opportune moment to advance with greater confidence toward their practical clinical applications. It is important to emphasize that achieving practical applications for microneedles necessitates addressing several critical criteria. Striking a balance among all factors related to microneedle preparation, including needle's shape, mechanical insertion performance, and the chosen fabrication platform, is a demanding task. All parameters associated with the microneedle platform, from design to fabrication, require robust justification.

Despite obstacles in transitioning from fundamental research to clinical practices, collaboration across scientific disciplines, including engineering, material sciences, and biomedicine, can pave a smoother path forward. Given the time-consuming and painful nature of many medical procedures, microneedles offer convenience, motivating the expedited transfer process. Expanding microneedles' applications into fields like theranostics, combining therapy and diagnosis, could lead to significant advancements, enhancing convenience and reducing costs. In recent years, there has been a notable emphasis on personalized medicine, aiming to tailor biomedical decisions to individual patients. Considering the significance of this objective, overcoming the limitations of a one-design-fits-all approach in microneedle preparation becomes crucial. Developing new microneedle designs aligns with the goals of personalized medicine, necessitating setups capable of high flexibility to create variants suited for specific applications.

Furthermore, integrating microneedle array systems with additional facilities, such as a camera or artificial intelligence-assisted equipment for real-time recording and analysis of therapeutic or biosensing processes, ensures efficient monitoring.[137] Given the small-scale of microneedles and their eventual application in the human body, ensuring reliable drug delivery or sensing platforms is essential.

Acknowledgements

N.K. acknowledges funding support from the Australian Research Council (ARC) Discovery Early Career Research Award (DECRA) DE220100205. N.-T.N. acknowledges funding support from the Australian Research

Council (ARC) through the Australian Laureate Fellowship (FL230100023) and ARC Discovery Project DP220100261.

Conflict of Interest

The authors declare no conflict of interest.

Keywords

biosensing, drug deliveries, microneedles, tissue adhesions

Received: March 17, 2024
Revised: July 22, 2024
Published online:

[1] E. Ece, I. Eş, F. Inci, *Mater. Today* **2023**, *68*, 275.
[2] Z. Faraji Rad, *Adv. Eng. Mater.* **2023**, *25*, 2201194.
[3] A. Kundu, M. G. Nogueira Campos, S. Santra, S. Rajaraman, *Sci. Rep.* **2019**, *9*, 14008.
[4] R. Omar, Y. Zheng, J. Wang, H. Haick, *Adv. Sens. Res.* **2023**, *2*, 2200032.
[5] X. Yi, Z. Yuan, X. Yu, L. Zheng, C. Wang, *ACS Appl. Mater. Interfaces* **2023**, *15*, 4873.
[6] N. Kashaninejad, A. Munaz, H. Moghadas, S. Yadav, M. Umer, N.-T. Nguyen, *Chemosensors* **2021**, *9*, 83.
[7] R. Zhang, Q. Miao, D. Deng, J. Wu, Y. Miao, Y. Li, *Colloids Surf., B* **2023**, *226*, 113302.
[8] J. Weng, G. Zheng, J. Wen, J. Yang, Q. Yang, X. Zheng, Q. Yan, *Drug Delivery* **2023**, *30*, 2232950.
[9] D. Terutsuki, R. Segawa, S. Kusama, H. Abe, M. Nishizawa, *J. Control. Release* **2023**, *354*, 694.
[10] H. Teymourian, F. Tehrani, K. Mahato, J. Wang, *Adv. Healthcare Mater.* **2021**, *10*, 2002255.
[11] J. Wang, Z. Lu, R. Cai, H. Zheng, J. Yu, Y. Zhang, Z. Gu, *Lab Chip* **2023**, *23*, 869.
[12] N. Kashaninejad, N.-T. Nguyen, *Lab Chip* **2023**, *23*, 913.
[13] H. Roh, Y. J. Yoon, J. S. Park, D.-H. Kang, S. M. Kwak, B. C. Lee, M. Im, *Nano-Micro Lett.* **2022**, *14*, 1.
[14] R. K. Haldkar, V. K. Gupta, T. Sheorey, *J. Mech. Sci. Technol.* **2017**, *31*, 2933.
[15] J. Y. Tan, A. Kim, J. J. Kim, *Appl. Phys. Lett.* **2021**, *119*, 023501.
[16] A. R. Johnson, C. L. Caudill, J. R. Tumbleston, C. J. Bloomquist, K. A. Moga, A. Ermoshkin, D. Shirvanyants, S. J. Mecham, J. C. Luft, J. M. DeSimone, *PLoS One* **2016**, *11*, e0162518.
[17] Z. Faraji Rad, R. E. Nordon, C. J. Anthony, L. Bilston, P. D. Prewett, J.-Y. Arns, C. H. Arns, L. Zhang, G. J. Davies, *Microsyst. Nanoeng.* **2017**, *3*, 1.
[18] A. Trautmann, G.-L. Roth, B. Nujiqi, T. Walther, R. Hellmann, *Microsyst. Nanoeng.* **2019**, *5*, 6.
[19] B. Jia, T. Xia, X. Wang, Y. Xu, Z. Guo, *J. Drug Delivery Sci. Technol.* **2023**, *88*, 104883.
[20] R. Ali, P. Mehta, M. Arshad, I. Kucuk, M. Chang, Z. Ahmad, *Aaps. Pharmscitech.* **2020**, *21*, 1.
[21] N.-W. Kang, S. Kim, J.-Y. Lee, K.-T. Kim, Y. Choi, Y. Oh, J. Kim, D.-D. Kim, J.-H. Park, *Expert Opin. Drug Delivery* **2021**, *18*, 929.
[22] H. Kathuria, D. Lim, J. Cai, B. G. Chung, L. Kang, *ACS Biomater. Sci. Eng.* **2020**, *6*, 5061.
[23] P. Pukfukdee, W. Banlunara, T. Rutwaree, B. Limcharoen, P. Sawutdeechaikul, T. Pattarakankul, T. Sansureerungsikul, P. Toprangkobsin, A. Leelahavanichkul, R. Panchaprateep, *ACS Appl. Bio Mater.* **2020**, *3*, 4581.
[24] S. H. Lim, W. J. Tiew, J. Zhang, P. C.-L. Ho, N. N. Kachouie, L. Kang, *Biofabrication* **2020**, *12*, 035003.
[25] C. Plamadeala, S. R. Gosain, F. Hischen, B. Buchroithner, S. Puthukodan, J. Jacak, A. Bocchino, D. Whelan, C. O'Mahony, W. Baumgartner, *Biomed. Microdevices* **2020**, *22*, 1.
[26] B. Z. Chen, L. Q. Zhang, Y. Y. Xia, X. P. Zhang, X. D. Guo, *Sci. Adv.* **2020**, *6*, eaba7260.
[27] G. Cole, A. A. Ali, C. M. McCrudden, J. W. McBride, J. McCaffrey, T. Robson, V. L. Kett, N. J. Dunne, R. F. Donnelly, H. O. McCarthy, *Eur. J. Pharm. Biopharm.* **2018**, *127*, 288.
[28] C. Ryall, S. Chen, S. Duarah, J. Wen, *Int. J. Pharm.* **2022**, *627*, 122221.
[29] K. Yi, Y. Wang, K. Shi, J. Chi, J. Lyu, Y. Zhao, *Biosens. Bioelectron.* **2021**, *190*, 113404.
[30] M. Sang, M. Cho, S. Lim, I. S. Min, Y. Han, C. Lee, J. Shin, K. Yoon, W.-H. Yeo, T. Lee, *Sci. Adv.* **2023**, *9*, eadh1765.
[31] S. N. Economidou, C. P. Pissinato Pere, M. Okereke, D. Douroumis, *Micromachines* **2021**, *12*, 117.
[32] Y. Mizuno, K. Takasawa, T. Hanada, K. Nakamura, K. Yamada, H. Tsubaki, M. Hara, Y. Tashiro, M. Matsuo, T. Ito, *Biomed. Microdevices* **2021**, *23*, 1.
[33] V. T. N. Linh, S.-G. Yim, C. Mun, J.-Y. Yang, S. Lee, Y. W. Yoo, D. K. Sung, Y.-I. Lee, D.-H. Kim, S.-G. Park, *Appl. Surf. Sci.* **2021**, *551*, 149411.
[34] M. Suzuki, T. Takahashi, S. Aoyagi, *Int. J. Nanotechnol.* **2018**, *15*, 157.
[35] H. Kim, J. Lee, U. Heo, D. K. Jayashankar, K.-C. Agno, Y. Kim, C. Y. Kim, Y. Oh, S.-H. Byun, B. Choi, *Sci. Adv.* **2024**, *10*, eadk5260.
[36] H. Ji, M. Wang, Y. Wang, Z. Wang, Y. Ma, L. Liu, H. Zhou, Z. Xu, X. Wang, Y. Chen, *npj Flex. Electron.* **2023**, *7*, 46.
[37] S. Chen, H. Matsumoto, Y. Moro-Oka, M. Tanaka, Y. Miyahara, T. Suganami, A. Matsumoto, *ACS Biomater. Sci. Eng.* **2019**, *5*, 5781.
[38] B. Newell, W. Zhan, *J. Control. Release* **2023**, *360*, 447.
[39] W. Shu, H. Heimark, N. Bertollo, D. J. Tobin, E. D. O'Cearbhaill, A. N. Annaidh, *Acta Biomater.* **2021**, *135*, 403.
[40] P. R. Yadav, L. J. Dobson, S. K. Pattanayek, D. B. Das, *Chem. Eng. Sci.* **2022**, *247*, 117005.
[41] C. Tarar, E. Aydın, A. K. Yetisen, S. Tasoglu, *ACS Omega* **2023**, *8*, 20968.
[42] P. R. Yadav, T. Han, O. Olatunji, S. K. Pattanayek, D. B. Das, *Pharmaceutics* **2020**, *12*, 693.
[43] P. Makvandi, A. Maleki, M. Shabani, A. R. Hutton, M. Kirkby, R. Jamaledin, T. Fang, J. He, J. Lee, B. Mazzolai, *Matter* **2022**, *5*, 390.
[44] R. Parhi, *J. Drug Delivery Sci. Technol.* **2022**, *75*, 103639.
[45] H. S. Lee, H. R. Ryu, J. Y. Roh, J.-H. Park, *Pharm. Res.* **2017**, *34*, 101.
[46] D. D. Zhu, Q. L. Wang, X. B. Liu, X. D. Guo, *Acta Biomater.* **2016**, *41*, 312.
[47] S. Fakhraei Lahiji, Y. Kim, G. Kang, S. Kim, S. Lee, H. Jung, *Sci. Rep.* **2019**, *9*, 7886.
[48] R. Jamaledin, P. Makvandi, C. K. Yiu, T. Agarwal, R. Vecchione, W. Sun, T. K. Maiti, F. R. Tay, P. A. Netti, *Adv. Therap.* **2020**, *3*, 2000171.
[49] S. Park, K. Lee, W. Ryu, *Expert Opin. Drug Delivery* **2022**, *19*, 1115.
[50] W. Li, R. N. Terry, J. Tang, M. R. Feng, S. P. Schwendeman, M. R. Prausnitz, *Nat. Biomed. Eng.* **2019**, *3*, 220.
[51] Y. Zhang, D. Chai, M. Gao, B. Xu, G. Jiang, *Int. J. Polym. Mater. Polym. Biomater.* **2019**, *68*, 850.
[52] H. Kim, H. S. Lee, Y. Jeon, W. Park, Y. Zhang, B. Kim, H. Jang, B. Xu, Y. Yeo, D. R. Kim, *ACS Nano* **2020**, *14*, 7227.
[53] F. Nazary Abrbekoh, L. Salimi, S. Saghati, H. Amini, S. Fathi Karkan, K. Moharamzadeh, E. Sokullu, R. Rahbarghazi, *J. Tissue Eng.* **2022**, *13*, 20417314221085390.

[54] N. Kashaninejad, E. Moradi, H. Moghadas, *Prog. Mol. Biol. Transl. Sci.* **2022**, *187*, 9.
[55] J. Ohn, M. Jang, B. M. Kang, H. Yang, J. T. Hong, K. H. Kim, O. Kwon, H. Jung, *Adv. Sci.* **2021**, *8*, 2004873.
[56] D. Huang, X. Fu, X. Zhang, Y. Zhao, *Research* **2022**, *2022*, 9809417.
[57] R. Liu, A. Li, Y. Lang, H. Cai, X. Tang, D. Li, X. Liu, J. Liu, *J. Drug Delivery Sci. Technol.* **2023**, *88*, 104922.
[58] Y. Hao, Y. Chen, X. He, F. Yang, R. Han, C. Yang, W. Li, Z. Qian, *Bioact. Mater.* **2020**, *5*, 542.
[59] Y. Xiang, J. Lu, C. Mao, Y. Zhu, C. Wang, J. Wu, X. Liu, S. Wu, K. Y. Kwan, K. M. Cheung, *Sci. Adv.* **2023**, *9*, eadf0854.
[60] J. Li, Y. Ma, D. Huang, Z. Wang, Z. Zhang, Y. Ren, M. Hong, Y. Chen, T. Li, X. Shi, *Nano-Micro Lett.* **2022**, *14*, 132.
[61] Y. Zhang, J. Yu, J. Wang, N. J. Hanne, Z. Cui, C. Qian, C. Wang, H. Xin, J. H. Cole, C. M. Gallippi, *Adv. Mater.* **2017**, *29*, 1604043.
[62] W. Chen, R. Tian, C. Xu, B. C. Yung, G. Wang, Y. Liu, Q. Ni, F. Zhang, Z. Zhou, J. Wang, *Nat. Commun.* **2017**, *8*, 1777.
[63] A. Ullah, H. Khan, H. J. Choi, G. M. Kim, *Polymers* **2019**, *11*, 1834.
[64] F. Rippke, E. Berardesca, T. M. Weber, *pH Skin: Issues Challenge.* **2018**, *54*, 87.
[65] X. Zhang, Y. Lin, R. J. Gillies, *J. Nucl. Med.* **2010**, *51*, 1167.
[66] X. Li, Q. Xu, P. Zhang, X. Zhao, Y. Wang, *J. Control. Release* **2019**, *314*, 72.
[67] H. Lu, S. Zada, L. Yang, H. Dong, *Front. Bioeng. Biotechnol.* **2022**, *10*, 851134.
[68] J. Xiao, S. Zhang, Q. Liu, T. Xu, X. Zhang, *Sensors Actuators, B* **2023**, *398*, 134685.
[69] A. Keirouz, Y. L. Mustafa, J. G. Turner, E. Lay, U. Jungwirth, F. Marken, H. S. Leese, *Small* **2023**, *19*, 2206301.
[70] G.-S. Liu, Y. Kong, Y. Wang, Y. Luo, X. Fan, X. Xie, B.-R. Yang, M. X. Wu, *Biomaterials* **2020**, *232*, 119740.
[71] J. J. García-Guzmán, C. Pérez-Ràfols, M. Cuartero, G. A. Crespo, *TrAC Trends Anal. Chem.* **2021**, *135*, 116148.
[72] Ö. Erdem, I. Eş, G. A. Akceoglu, Y. Saylan, F. Inci, *Biosensors* **2021**, *11*, 296.
[73] Z. Wang, J. Luan, A. Seth, L. Liu, M. You, P. Gupta, P. Rathi, Y. Wang, S. Cao, Q. Jiang, *Nat. Biomed. Eng.* **2021**, *5*, 64.
[74] S. Kim, M. S. Lee, H. S. Yang, J. H. Jung, *Sci. Rep.* **2021**, *11*, 14018.
[75] F. Leng, M. Zheng, C. Xu, *Exploration* **2021**, *1*, 20210109.
[76] M. Dervisevic, N. H. Voelcker, *ACS Mater. Lett.* **2023**, *5*, 1851.
[77] S. Y. Yang, E. D. O'Cearbhaill, G. C. Sisk, K. M. Park, W. K. Cho, M. Villiger, B. E. Bouma, B. Pomahac, J. M. Karp, *Nat. Commun.* **2013**, *4*, 1702.
[78] S. W. Chew, A. H. Shah, M. Zheng, H. Chang, C. Wiraja, T. W. Steele, C. Xu, *Bioeng. Transl. Med.* **2020**, *5*, e10157.
[79] S. Lim, T. Y. Park, E. Y. Jeon, K. I. Joo, H. J. Cha, *Biomaterials* **2021**, *278*, 121171.
[80] T. Li, J. Li, Z. Wang, Y. Ren, Y. Jin, D. Huang, Q. Wang, Z. Li, in *2021 IEEE 34th Inter. Conf. on Micro Electro Mechanical Systems (MEMS)*, IEEE, Piscataway, NJ **2021**, pp. 18–21.
[81] J. Gan, X. Zhang, W. Ma, Y. Zhao, L. Sun, *Nano Today* **2022**, *47*, 101630.
[82] T. Zhu, X. Yu, X. Yi, X. Guo, L. Li, Y. Hao, W. Wang, *Pharmaceutics* **2022**, *14*, 686.
[83] X. Zhang, Y. Wang, J. Chi, Y. Zhao, *Research* **2020**, *2020*, 7462915.
[84] L.-G. Tran, T.-Q. Nguyen, W.-T. Park, in *2019 IEEE 32nd Inter. Conf. on Micro Electro Mechanical Systems (MEMS)*, IEEE, Piscataway, NJ **2019**, pp. 547–550.
[85] Z. Sun, T. Liao, W. Li, Y. Qiao, K. Ostrikov, *Adv. Funct. Mater.* **2019**, *29*, 1901460.
[86] J. Yu, Y. Wang, S. Qin, G. Gao, C. Xu, Z. L. Wang, Q. Sun, *Mater. Today* **2022**, *60*, 158.
[87] E. Kizilkan, J. Strueben, A. Staubitz, S. N. Gorb, *Sci. Robot.* **2017**, *2*, eaak9454.
[88] F. Zhang, Z. Guo, *Mater. Adv.* **2020**, *1*, 2592.
[89] J. Lu, C.-V. Ngo, S. C. Singh, J. Yang, W. Xin, Z. Yu, C. Guo, *Langmuir* **2019**, *35*, 3562.
[90] Z. Han, Z. Mu, B. Li, Z. Wang, J. Zhang, S. Niu, L. Ren, *ACS Nano* **2016**, *10*, 8591.
[91] M. Li, T. Yang, Q. Yang, Z. Fang, H. Bian, C. Zhang, X. Hou, F. Chen, *Adv. Opt. Mater.* **2022**, *10*, 2200861.
[92] H. H. Vu, N. T. Nguyen, N. Kashaninejad, *Adv. Mater. Technol.* **2023**, *8*, 2201836.
[93] Q. Yin, Q. Guo, Z. Wang, Y. Chen, H. Duan, P. Cheng, *ACS Appl. Mater. Interfaces* **2020**, *13*, 1979.
[94] Y. Si, Z. Dong, L. Jiang, *ACS Cent. Sci.* **2018**, *4*, 1102.
[95] S. Liu, S. Chu, G. E. Banis, L. A. Beardslee, R. Ghodssi, in *2020 IEEE 33rd Inter. Conf. on Micro Electro Mechanical Systems (MEMS)*, IEEE, Piscataway, NJ **2020**, pp. 885–888.
[96] Y. Lu, T. Ren, H. Zhang, Q. Jin, L. Shen, M. Shan, X. Zhao, Q. Chen, H. Dai, L. Yao, *Acta Biomater.* **2022**, *153*, 386.
[97] T. Liu, Y. Sun, G. Jiang, W. Zhang, R. Wang, L. Nie, A. Shavandi, K. E. Yunusov, U. E. Aharodnikau, S. O. Solomevich, *Acta Biomater.* **2023**, *160*, 32.
[98] X. Fu, X. Zhang, D. Huang, L. Mao, Y. Qiu, Y. Zhao, *Chem. Eng. J.* **2022**, *431*, 133362.
[99] M. Amer, R. K. Chen, *Macromol. Biosci.* **2020**, *20*, 2000089.
[100] M. Amer, X. Ni, M. Xian, R. K. Chen, *J. Eng. Sci. Med. Diagnostics Therapy* **2022**, *5*, 011001.
[101] S. Yao, Y. Luo, Y. Wang, *Eng. Regeneration* **2022**, *3*, 232.
[102] Y. Deng, C. Yang, Y. Zhu, W. Liu, H. Li, L. Wang, W. Chen, Z. Wang, L. Wang, *Nano Lett.* **2022**, *22*, 2702.
[103] J. Xu, R. Danehy, H. Cai, Z. Ao, M. Pu, A. Nusawardhana, D. Rowe-Magnus, F. Guo, *ACS Appl. Mater. Interfaces* **2019**, *11*, 14640.
[104] R. Jamaledin, C. K. Yiu, E. N. Zare, L. N. Niu, R. Vecchione, G. Chen, Z. Gu, F. R. Tay, P. Makvandi, *Adv. Mater.* **2020**, *32*, 2002129.
[105] X. Zhang, G. Chen, L. Sun, F. Ye, X. Shen, Y. Zhao, *Chem. Eng. J.* **2021**, *406*, 126741.
[106] M. Rajabi, N. Roxhed, R. Z. Shafagh, T. Haraldson, A. C. Fischer, W. V. D. Wijngaart, G. Stemme, F. Niklaus, *PLoS One* **2016**, *11*, e0166330.
[107] A. Sadeqi, G. Kiaee, W. Zeng, H. Rezaei Nejad, S. Sonkusale, *Sci. Rep.* **2022**, *12*, 1853.
[108] J. Lee, E. H. Jang, J. H. Kim, S. Park, Y. Kang, S. Park, K. Lee, J.-H. Kim, Y.-N. Youn, W. Ryu, *J. Control. Release* **2021**, *340*, 125.
[109] M. Avcil, A. Çelik, *Micromachines* **2021**, *12*, 1321.
[110] V. Ebrahiminejad, P. D. Prewett, G. J. Davies, Z. Faraji Rad, *Adv. Mater. Interfaces* **2022**, *9*, 2101856.
[111] B. Ahn, *Int. J. Control Autom. Syst.* **2020**, *18*, 143.
[112] M. Razzaghi, M. Akbari, *Micromachines* **2023**, *14*, 1157.
[113] Y. Cai, S. Huang, Z. Zhang, J. Zhang, X. Zhu, X. Chen, X. Ding, *Research* **2022**, *2022*, 9869734.
[114] S. Lee, S. Fakhraei Lahiji, J. Jang, M. Jang, H. Jung, *Pharmaceutics* **2019**, *11*, 402.
[115] E. L. Zoudani, M. Soltani, *Eur. J. Pharm. Sci.* **2020**, *150*, 105339.
[116] H. S. Min, Y. Kim, J. Nam, H. Ahn, M. Kim, G. Kang, M. Jang, H. Yang, H. Jung, *Biomater. Adv.* **2023**, *145*, 213248.
[117] X. Luo, L. Yang, Y. Cui, *Biomed. Microdevices* **2023**, *25*, 20.
[118] S. Machekposhti, M. Soltani, P. Najafizadeh, S. Ebrahimi, P. Chen, *J. Control. Release* **2017**, *261*, 87.

[119] G. Bonfante, H. Lee, L. Bao, J. Park, N. Takama, B. Kim, *Micro Nano Syst. Lett.* **2020**, *8*, 1.
[120] I. Papautsky, E. T. K. Peterson, *Encyclopedia of Microfluidics and Nanofluidics* (Ed: D. Li), Springer US, Boston, MA **2008**, pp. 1256–1267.
[121] X. Zhang, G. Chen, L. Cai, Y. Wang, L. Sun, Y. Zhao, *Chem. Eng. J.* **2021**, *414*, 128905.
[122] X. Zhang, F. Wang, Y. Yu, G. Chen, L. Shang, L. Sun, Y. Zhao, *Sci. Bull.* **2019**, *64*, 1110.
[123] M. Zukerstein, J. Hrabovsky, J. Sladek, I. Mirza, Y. Levy, N. Bulgakova, *Appl. Surf. Sci.* **2022**, *592*, 153228.
[124] M. Guo, Y. Wang, B. Gao, B. He, *ACS Nano* **2021**, *15*, 15316.
[125] Y. Wang, B. Gao, B. He, *Small* **2023**, *19*, 2206270.
[126] S. Mckee, A. Lutey, C. Sciancalepore, F. Poli, S. Selleri, A. Cucinotta, *J. Photochem. Photobiol. B* **2022**, *229*, 112424.
[127] X. Li, W. Shan, Y. Yang, D. Joralmon, Y. Zhu, Y. Chen, Y. Yuan, H. Xu, J. Rong, R. Dai, *Adv. Funct. Mater.* **2021**, *31*, 2003725.
[128] Z. Faraji Rad, P. D. Prewett, G. J. Davies, *Microsyst. Nanoeng.* **2021**, *7*, 71.
[129] B. Szeto, A. Aksit, C. Valentini, M. Yu, E. G. Werth, S. Goeta, C. Tang, L. M. Brown, E. S. Olson, J. W. Kysar, *Hear. Res.* **2021**, *400*, 108141.
[130] D. Han, R. S. Morde, S. Mariani, A. A. La Mattina, E. Vignali, C. Yang, G. Barillaro, H. Lee, *Adv. Funct. Mater.* **2020**, *30*, 1909197.
[131] S. S. Deshmukh, A. Goswami, *Mater. Today: Proc.* **2020**, *26*, 405.
[132] J. Li, Y. Zhou, J. Yang, R. Ye, J. Gao, L. Ren, B. Liu, L. Liang, L. Jiang, *Mater. Sci. Eng. C* **2019**, *96*, 576.
[133] S. Henry, D. V. McAllister, M. G. Allen, M. R. Prausnitz, *J. Pharm. Sci.* **1998**, *87*, 922.
[134] S. Lyu, Z. Dong, X. Xu, H.-P. Bei, H.-Y. Yuen, C.-W. J. Cheung, M.-S. Wong, Y. He, X. Zhao, *Bioact. Mater.* **2023**, *27*, 303.
[135] O. Howells, G. J. Blayney, B. Gualeni, J. C. Birchall, P. F. Eng, H. Ashraf, S. Sharma, O. J. Guy, *Eur. J. Pharm. Biopharm.* **2022**, *171*, 19.
[136] Z. Chen, Y. Lin, W. Lee, L. Ren, B. Liu, L. Liang, Z. Wang, L. Jiang, *ACS Appl. Mater. Interfaces* **2018**, *10*, 29338.
[137] S. N. Economidou, M. J. Uddin, M. J. Marques, D. Douroumis, W. T. Sow, H. Li, A. Reid, J. F. Windmill, A. Podoleanu, *Addit. Manuf.* **2021**, *38*, 101815.
[138] K. T. Tran, T. D. Gavitt, N. J. Farrell, E. J. Curry, A. B. Mara, A. Patel, L. Brown, S. Kilpatrick, R. Piotrowska, N. Mishra, *Nat. Biomed. Eng.* **2021**, *5*, 998.
[139] S. Yao, Y. Wang, J. Chi, Y. Yu, Y. Zhao, Y. Luo, Y. Wang, *Adv. Sci.* **2022**, *9*, 2103449.
[140] Q. Li, R. Xu, H. Fan, J. Xu, Y. Xu, P. Cao, Y. Zhang, T. Liang, Y. Zhang, W. Chen, *ACS Nano* **2022**, *16*, 7512.
[141] C. Song, X. Zhang, M. Lu, Y. Zhao, *Research* **2023**, *6*, 0119.
[142] X. Zhang, G. Chen, Y. Yu, L. Sun, Y. Zhao, *Research* **2020**, *2020*, 3672120.
[143] X. Zhang, X. Fu, G. Chen, Y. Wang, Y. Zhao, *Adv. Sci.* **2021**, *8*, 2101210.
[144] S. De Martino, M. Battisti, F. Napolitano, A. Palladino, L. Serpico, E. Amendola, A. Martone, P. De Girolamo, A. Squillace, P. Dardano, *Biomater. Adv.* **2022**, *142*, 213169.
[145] X. Zhang, J. Gan, L. Fan, Z. Luo, Y. Zhao, *Adv. Mater.* **2023**, *35*, 2210903.
[146] C. Caudill, J. L. Perry, K. Iliadis, A. T. Tessema, B. J. Lee, B. S. Mecham, S. Tian, J. M. DeSimone, *Proc. Natl Acad. Sci.* **2021**, *118*, e2102595118.
[147] J. Lim, D. Tahk, J. Yu, D.-H. Min, N. L. Jeon, *Microsyst. Nanoeng.* **2018**, *4*, 29.
[148] X. Huang, S. Zheng, B. Liang, M. He, F. Wu, J. Yang, H.-J. Chen, X. Xie, *Microsyst. Nanoeng.* **2023**, *9*, 25.

Elham Lori Zoudani received both her bachelor's and master's degrees in mechanical engineering from Shahid Chamran University (SCU), and Khaje Nasir Toosi University of Technology (KNTU), Iran, in 2015 and 2019, respectively. In 2023, she joined Queensland Micro- and Nanotechnology Centre (QMNC) at Griffith University, Australia, as a Ph.D. candidate. Her research focuses on microneedle design and development for biomedical applications. Her research interests are microfluidics, biomedical microdevices, and computational fluid dynamics.

Nam-Trung Nguyen received his Dip-Ing., Dr. Ing., and Dr. Ing. Habil degrees from Chemnitz University of Technology, Germany, in 1993, 1997, and 2004, respectively. From 1999 to 2013, he was an associate professor at Nanyang Technological University, Singapore. From 2013 to 2023, he was a professor and director of Queensland Micro- and Nanotechnology Centre at Griffith University, Australia. In 2023, he was awarded the Australian Laureate Fellowship for advancing the field of microfluidics. He is a fellow of ASME and a senior member of IEEE. He is also an elected fellow of American Society of Mechanical Engineers.

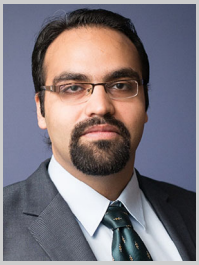

Navid Kashaninejad received his Ph.D. from Nanyang Technological University (NTU), Singapore, under the prestigious SINGA scholarship. He has extensive experience in designing and fabricating microfluidic devices for biomedical applications, including cancer treatment. In 2021, he was awarded the DECRA fellowship, recognizing his significant contributions. Currently, he is pioneering the emerging field of surface microfluidics, working to establish and advance its applications. His research focuses on innovative fabrication techniques and complex surface interactions. These contributions are poised to make a substantial impact across a range of applications, from advanced microfluidic devices to cutting-edge biosensing technologies.